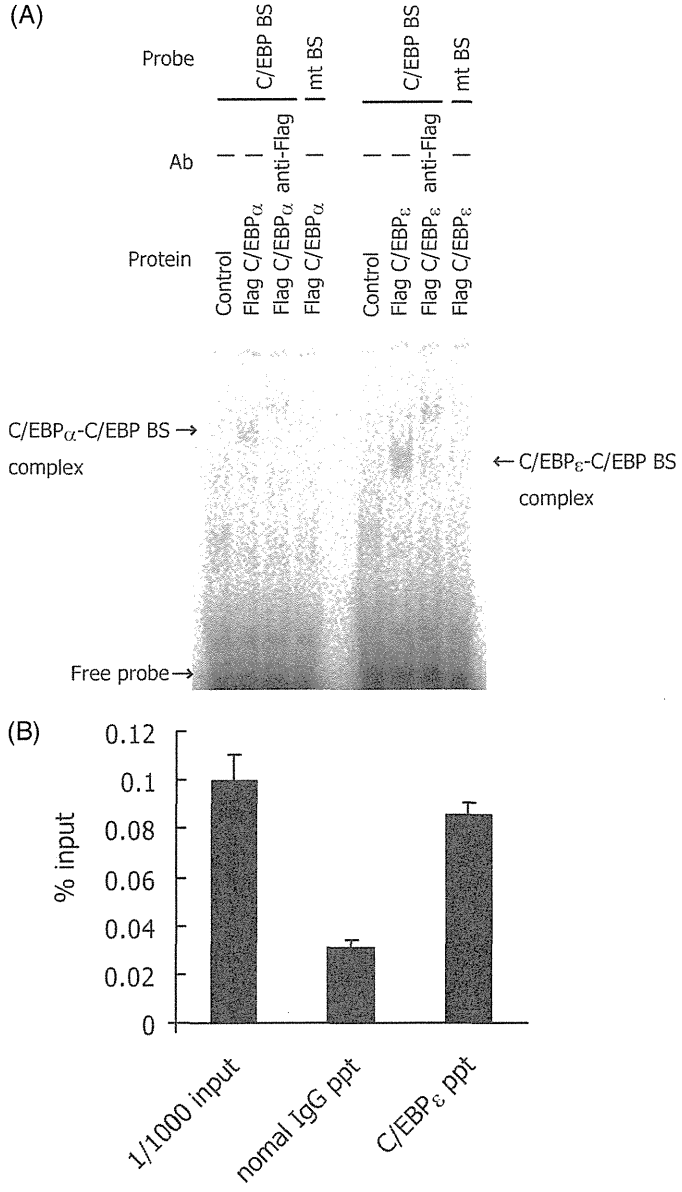

FIGURE 3. **Binding of C/EBPα and -ϵ to the binding site in the LMP1 *ED-L1* promoter.** *A*, EMSA was carried out as described under "Experimental Procedures." FLAG-tagged C/EBPα (*left panel*) or ϵ (*right panel*) were produced *in vitro* and incubated with ^{32}P-labeled wild-type (*C/EBP BS*) or point-mutated (*mtBS*) probe. Supershift analysis was performed using mouse anti-FLAG monoclonal antibodies. The samples were then separated in a 4% polyacrylamide gel and analyzed with Fuji Image Analyzer BAS2500. *B*, binding of endogenous C/EBPϵ to *LMP1* promoter. AGS-CR2/GFP-EBV-Bac cells, latently infected with EBV, were subjected to ChIP assays using anti-C/EBPϵ antibody (Santa Cruz), followed by real time PCR analysis for quantification.

assays revealed that C/EBPα-mediated transactivation was severely attenuated when the putative motif at −268 was mutated, whereas replacement of the other two possible motifs did not cause any defect (Fig. 2*D*). These results suggest that the ATTGCCGCAC motif at the −268 of ED-L1 promoter is the *cis*-element responsible for the response to C/EBP.

We then used EMSA to examine whether the C/EBP protein could actually bind to the ATTGCCGCAC motif at −268 in the *ED-L1* promoter (Fig. 3*A*). Addition of FLAG-tagged C/EBPα or -ϵ produced a specific band for the C/EBP-nucleotide complex when the wild-type C/EBP binding site at the −268 of *ED-L1* (C/EBP BS) sequence was used, whereas this failed to be produced with mtC/EBP BS, the mutated sequence. Supershift analysis with anti-FLAG antibody demonstrated that the band actually contained FLAG-tagged C/EBP protein. Therefore, C/EBP binds to the ATTGCCGCAC motif in question.

We also tried to detect binding of endogenous C/EBP to the *LMP1* promoter. In AGS-CR2/GFP-EBV-Bac cells, C/EBPϵ was detected on the promoter sequence (Fig. 3*B*), although C/EBPα was undetectable (not shown). Because the amount of C/EBPα is very low in the cell line, we speculate that the ChIP result simply reflects the expression level of the family member.

Previous reports demonstrated that a distal promoter, termed *TR-L1*, located within the TR of the viral genome, is also activated in addition to the proximal *ED-L1* promoter in certain cell types with EBNA2-independent *LMP1* expression (10, 13, 15, 16), we next examined, by RT-PCR, if C/EBP might affect the *TR-L1* promoter, too. An antisense primer was designed to jump the first intron of the *LMP1* gene (Fig. 4*A*, primer *3*), so that the possibility of genomic contamination could be ignored, and one sense primer was set within the first exon (Fig. 4*A*, primer *1*) and another sense set well upstream of the transcription start site (+1) of the *ED-L1* promoter (Fig. 4*A*, primer *2*). The result of the RT-PCR (Fig. 4*B*) indicated that C/EBPα markedly enhanced transcription from the *TR-L1* promoter. It is not clear, from this result, whether the *ED-L1* promoter is also activated or not.

Although we already identified the *cis*-element responsible for activation of the proximal *ED-L1* promoter (Fig. 2), we then searched to find the *cis*-element that is crucial for the activation of the distal promoter, because the *TR-L1* promoter of the *LMP1* gene was markedly activated by C/EBPα (Fig. 4). We first prepared a firefly luciferase reporter construct by inserting the *TR-L1* promoter (nucleotide −1115 to −544, Fig. 5*A*, *TR*). Curiously, this reporter did not respond to exogenous expression of C/EBPα (Fig. 5*B*, TR), suggesting that a functional *cis*-element responsible for activation of the *TR-L1* promoter does not exist in the sequence between nucleotides −1115 and −544. Therefore, speculating that the C/EBP binding site located within the *ED-L1* promoter might act to influence the *TR-L1* promoter activity form downstream, the promoter sequence in the reporter construct was extended to −147, to cover the C/EBP motif (Fig. 5*A*, *TR+BS*). Although this reporter contains part of the *ED-L1* promoter, transcription from ED-L1 should not initiate because it does not contain the transcription start site (+1) of the ED-L1 promoter. As shown in Fig. 5*B* (*TR+BS*), the vector did respond to C/EBPα, and introduction of a point mutation at the C/EBP BS depressed the response (Fig. 5*C*, *TR+BSmt*). In addition, a reporter containing the *TR-L1* and complete *ED-L1* promoters (Fig. 5*A*, *TR+ED*) acted in a similar manner (Fig. 5*D*, *TR+ED* and *TR+EDmt*). These results suggest that activation of both the *TR-L1* and *ED-L1* promoters by C/EBP is mediated through the single C/EBP binding site in the *ED-L1* promoter.

Mutation in the C/EBP Binding Site Attenuated Activity of Both LMP1 Promoters in the Context of the Viral Genome—Experiments so far have indicated there is one functional C/EBP binding site in the *ED-L1* promoter through which activation of both *ED-L1* and *TR-L1* promoters is mediated. To further

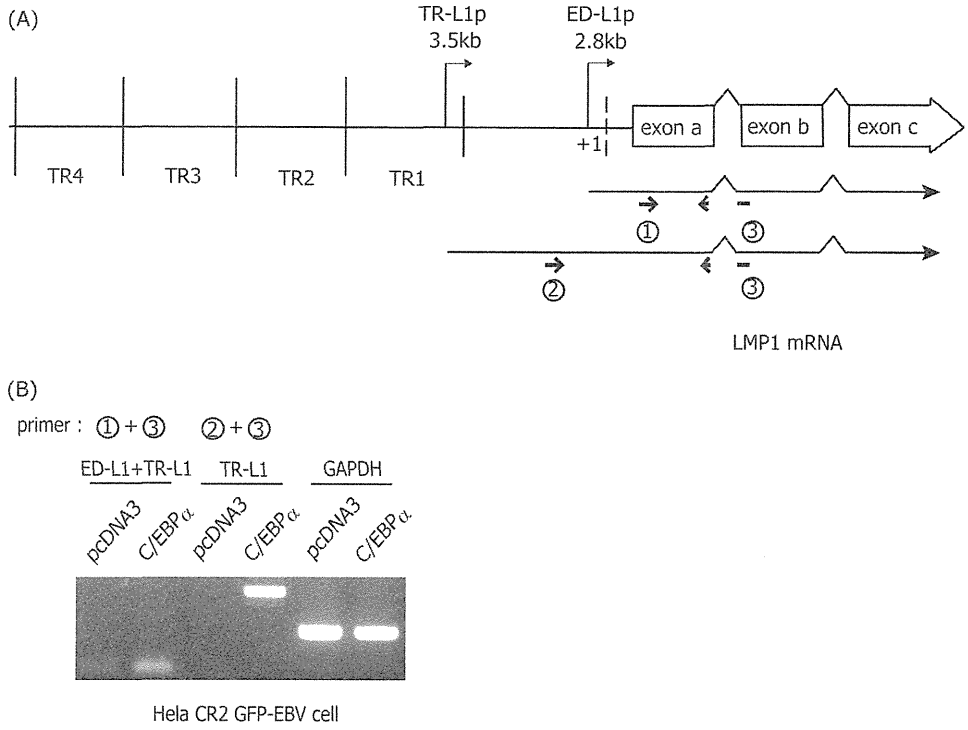

FIGURE 4. **Activation of the *LMP1 TR-L1* promoter by C/EBPα in cells latently infected with EBV.** *A*, schematic representation of the regulatory sequence of the *LMP1* gene. The 2.8- and 3.5-kb *LMP1* mRNAs and the primers used for RT-PCR in *B* are depicted. *B*, HeLa-CR2/GFP-EBV cells were transfected with empty vector (*pcDNA3*) or the indicated C/EBPα expression vector. After 60 h, cell RNAs were harvested and subjected to RT-PCR using the primers indicated above.

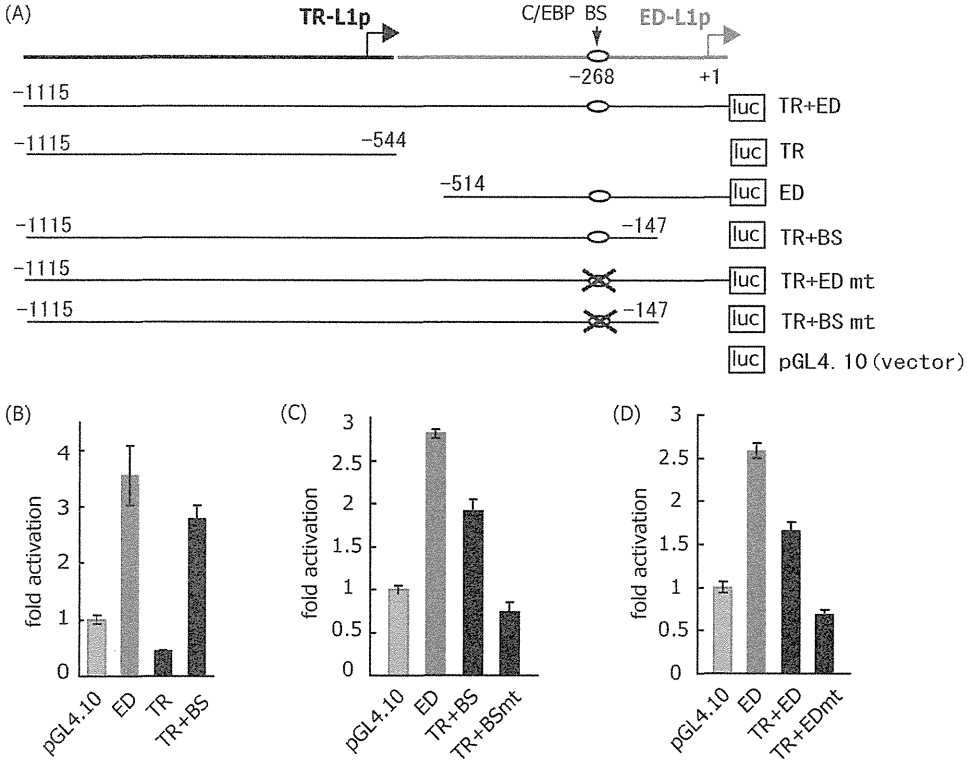

FIGURE 5. **Identification of the sequence motif responsible for activation of the *LMP1 TR-L1* promoter by C/EBPα.** *A*, schematic representation of reporter constructs with truncated and/or mutated *LMP1* promoter sequences. Identified C/EBP binding sites in the *ED-L1* promoter are *ringed*. *B*, the C/EBPα expression plasmid or its empty vector were cotransfected into HEK293T cells with the mutated reporter plasmid in *A* and pCMV-RLuc. Luciferase assays were carried out after 1 day as described under "Experimental Procedures." Firefly luciferase activity was normalized to *Renilla* luciferase activity. *Bars* indicate averages of fold-activation by transfection of C/EBPα, compared with those with the empty vector, and S.D., for each reporter. The *numbers* in the figure indicate nucleotide positions relative to the transcription start site (+1).

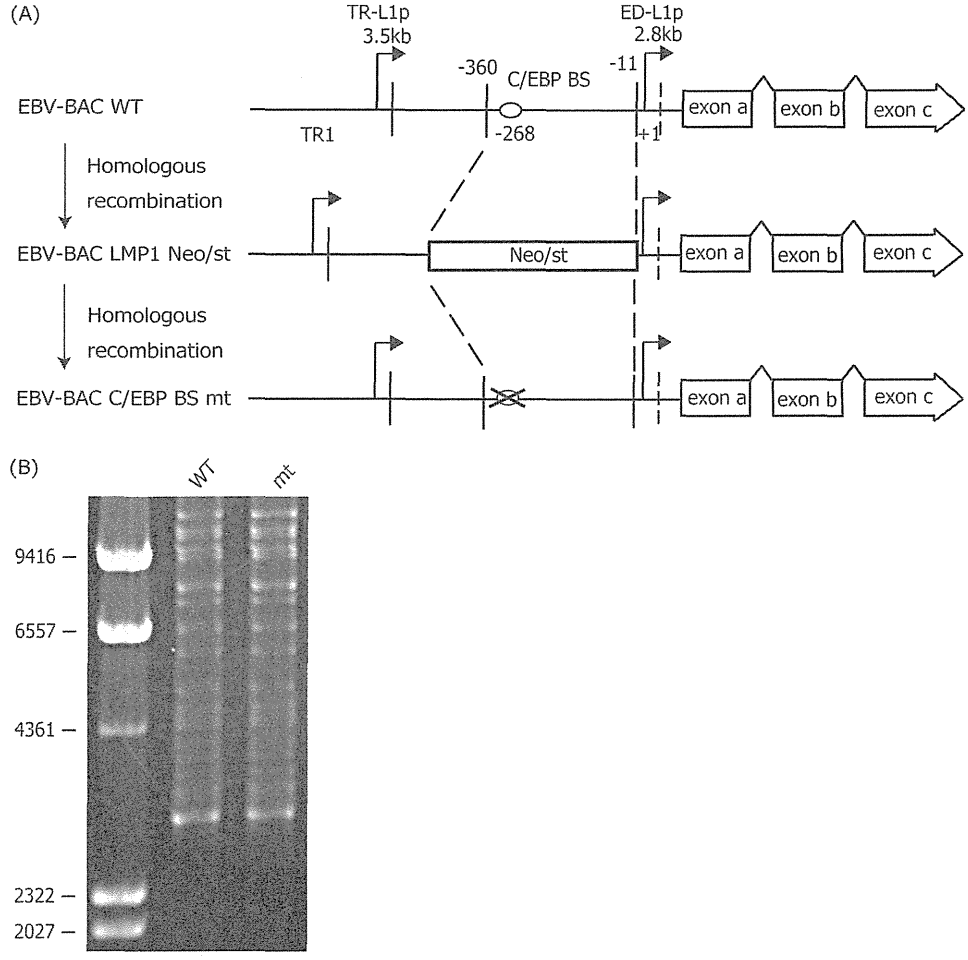

FIGURE 6. **Construction of a recombinant EBV featuring point mutation in the C/EBP binding site of the *LMP1* promoter.** *A*, schematic arrangement of the recombination of the EBV genome using the tandemly arranged neomycin-resistance and streptomycin-sensitivity genes (*Neo/st*). The sequences around the C/EBP binding site (C/EBP BS, *ringed*) of the B95-8 *LMP1* promoter (−360 to −11) were first replaced with the Neo/st cassette, which was then replaced with a point mutated C/EBP BS sequence (*ringed X*) to construct EBV-BAC C/EBP BS mt. *B*, electrophoresis of the recombinant viruses. The recombinant EBV genomes were digested with BamHI and separated in an agarose gel.

extend and verify the findings, recombinant EBV with a point mutation at the identified C/EBP binding site was prepared. As shown in Fig. 6*A*, part of the *LMP1 ED-L1* promoter sequence (−360 to −11), containing the C/EBP binding site (C/EBP BS, *ringed* in Fig. 6*A*), was first replaced with the marker cassette (Neo/st), and then this was exchanged with the mutated C/EBP binding site (C/EBP BSmt) sequence, to prepare EBV-BAC C/EBP BSmt. Sequencing analysis confirmed that the EBV-BAC C/EBP BSmt DNA had the same mutation as the pLMP1/−268mt-FLuc vector (Fig. 2*C*), as intended. Integrity of the BAC DNA was checked by BamHI digestion followed by electrophoresis to confirm that the recombinant viruses did not carry obvious deletions or insertions (Fig. 6*B*). Recombinant EBV-BAC DNA was introduced into a virus-producing cell line, HEK293, followed by hygromycin selection, to establish cell lines in which multiple copies were maintained as an episome. More than 10 cell colonies from each recombinant virus were obtained and viral protein expression levels in the presence and absence of BZLF1 inductions were examined. The recombinant virus was then infected into AGS-CR2, expressing the cellular receptor for EBV, CR2 (CD21).

Protein levels were examined in the AGS cells, latently infected with wild-type or mutated EBV (Fig. 7*A*). Production of the LMP1 protein in the AGS cells with virus carrying the point mutation at the C/EBP binding site (Fig. 7*A*, *mt*) was obviously lower than in the wild-type. The AGS cells expressed little or no EBNA2, in contrast to the lymphoblastoid cell line (Fig. 7*A*), indicating that the virus established type II latency in the cells (31). Promoter usage patterns were then checked by RT-PCR using the specific primers used for Fig. 4. Transcription from the *TR-L1* promoter was remarkably restricted with the mutant (Fig. 7*B*), although the effect of the mutation on the *ED-L1* promoter was not distinguishable from the data. We also checked that EBNA1 levels were comparable (Fig. 7, *A* and *B*).

Next, the effects of C/EBP exogenous expression were analyzed in cells carrying recombinant viruses. In AGS cells latently infected with wild-type EBV, intrinsic LMP1 protein was present and ectopic supply of C/EBPα caused a prominent increase in LMP1 protein levels (Fig. 7*C*). On the other hand, in cells with mutant EBV, the intrinsic LMP1 protein level was low and C/EBPα expression did not induce an increase (Fig. 7*C*). RT-PCR analysis clearly showed that transcriptional activation of the *LMP1* gene by C/EBPα in wild-type, at least for the *TR-L1* promoter, was diminished in the mutant (Fig. 7*D*), indicating significance for the motif.

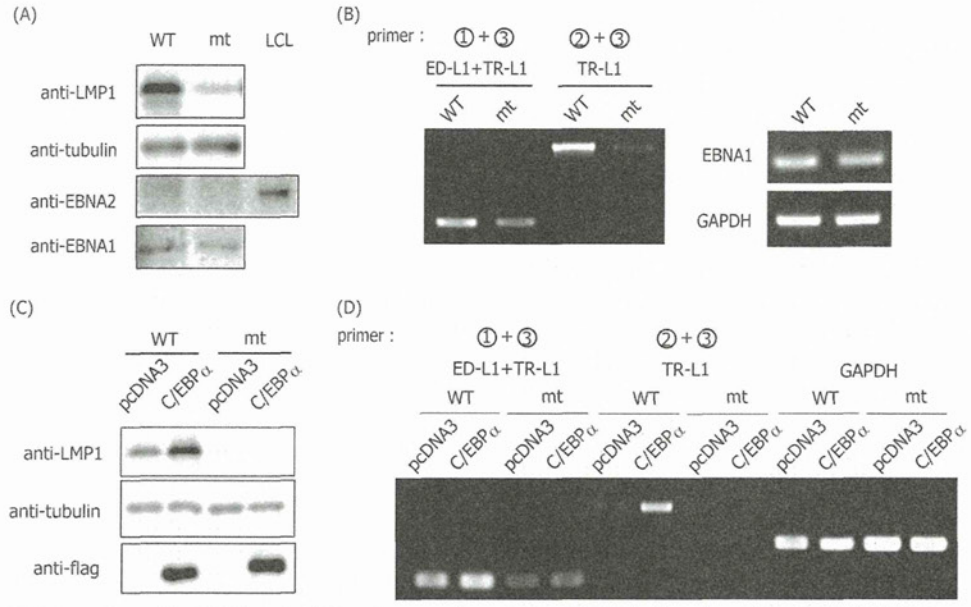

FIGURE 7. **Decrease in LMP1 protein and mRNA levels with point mutation of the C/EBP binding site of the EBV-BAC *LMP1* promoter.** *A*, LMP1 protein levels in AGS cells latently infected with wild-type or point-mutated EBV-BAC. Immunoblotting was performed using anti-LMP1, -tubulin, and -EBNA2 antibodies. Proteins from the lymphoblastoid cell line were also included as a positive control for EBNA2. *B*, both *TR-L1* and *ED-L1* promoters were attenuated by point mutation of the C/EBP binding site of EBV-BAC *LMP1* promoter. RNA was collected from AGS cells latently infected with wild-type or point-mutated EBV-BAC, and subjected to RT-PCR using the primers shown in Fig. 5*A*. *EBNA1* and *GAPDH* levels were also checked. *C*, response to ectopic expression of C/EBPα was diminished by point mutation of the C/EBP binding site of EBV-BAC *LMP1* promoter. AGS cells latently infected with wild-type or point-mutated EBV-BAC were transfected with the C/EBPα expression vector or its empty vector (*pcDNA3*). After 60 h, cell proteins were harvested and subjected to immunoblotting with anti-LMP1, -tubulin, and -FLAG antibodies. *D*, responses of both *TR-L1* and *ED-L1* promoters to ectopic expression of C/EBPα were diminished by point mutation of the C/EBP binding site of EBV-BAC *LMP1* promoter. AGS cells latently infected with wild-type or point-mutated EBV-BAC were transfected with C/EBPα expression vector or its empty vector (*pcDNA3*). After 60 h, RNA was collected and subjected to RT-PCR using the primers shown in Fig. 4*A*.

Knockdown of C/EBP Reduced LMP1 Levels—Last, we tested the effect of endogenous C/EBP proteins on LMP1 expression levels. To this end, α or ϵ members of the C/EBP family were ablated by shRNA technology. In HeLa-CR2/GFP-EBV cells, knockdown of either C/EBPα or -ϵ significantly restricted the amount of LMP1 (Fig. 8*A* and supplemental Fig. S3). In AGS-CR2/GFP-EBV-Bac cells, we tested knockdown of C/EBPϵ. Because levels of endogenous C/EBPα in the cells were very low, knockdown of C/EBPα was not done. Treatment of shC/EBPϵ also caused reduction of LMP1 protein in AGS cells (Fig. 8*B*). These results indicate that C/EBP proteins are involved in LMP1 production, and suggest that the effect is dependent on cell types.

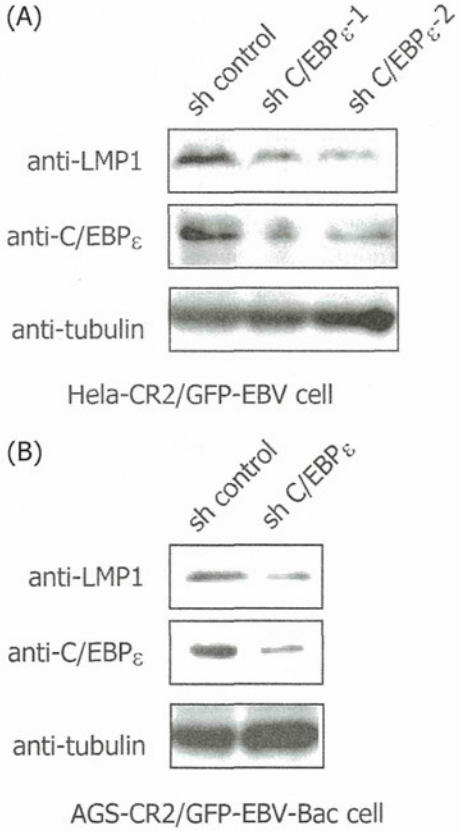

FIGURE 8. **Knockdown of C/EBPϵ decreased levels of LMP1.** HeLa-CR2/GFP-EBV (*A*) and AGS-CR2/GFP-EBV-Bac (*B*) cells were treated with control shRNA or shRNA for the C/EBPϵ. Cell proteins were harvested and subjected to immunoblotting with anti-LMP1, -C/EBPϵ, and -tubulin antibodies.

DISCUSSION

The results documented here show clear involvement of C/EBP proteins in up-regulation of the *LMP1* gene. Initially, the C/EBPϵ protein was identified by our screening to increase the proximal *LMP1* (*ED-L1*) promoter activity. We are confident in the screening system, because factors like SP3- and Ets-type transcription factors, both of which have been implicated in the transcriptional regulation of *LMP1*, were isolated in the screen. Regarding Ets transcription factors, PU.1 has been reported to recruit the viral transcriptional activator EBNA2 and thereby enhance *LMP1 ED-L1* promoter activity (5, 6), but it is understandable that PU.1 up-regulated transcription even without EBNA2 in the screening experiment, because PU.1 can functionally interact with basic transcriptional regulators, like CBP, TFIID, or TBP, or other transcription factors, like GATA or RUNX (32, 33). Another Ets family transcription factor FLI1

was also identified in our screening. Interestingly, whereas FLI1 markedly elicited promoter activity (about 40–50-fold) in the reporter assays, exogenous expression of FLI1 did not cause an increase in the levels of LMP1 protein in EBV-positive cells (data not shown). Likewise, PU.1 also did not significantly augment the LMP1 protein levels (data not shown). On the other hand, whereas the increment of the reporter activity by C/EBPϵ was not very high (only 2–4-fold), exogenous expression of the gene clearly increased the mRNA and protein levels of LMP1 in EBV-positive cells (Figs. 1, *B* and *C*, 4, and supplemental Fig. S2). Therefore, we must conclude that transient reporter assays do not always reflect the actual promoter activity in the context of viral genome. The reason why overexpression of the Ets family transcription factors fail to increase the LMP1 protein levels in the context of infection is not clear. We speculate either that the promoter might already be occupied with certain Ets family proteins, or that the ability of the FLI1 or PU.1 to enhance the promoter activity might not be sufficiently strong as to counter epigenetic suppression of the gene but high enough for reporter assays.

Subsequent analyses demonstrated that C/EBP enhanced the distal *TR-L1* promoter of *LMP1*, and that the activation was mediated through one C/EBP binding motif in the proximal *ED-L1* promoter (supplemental Fig. S4). Therefore, the distal *TR-L1* promoter is activated by C/EBP binding downstream of the transcription start site of the *TR-L1* promoter. Because activation of a particular promoter by transcription factor binding downstream of the transcription start site has been demonstrated previously for various promoters (34, 35), we assume the activation of the *TR-L1* promoter by downstream C/EBP binding is reasonable when considered in light of our clear results of reporter assays and the point-mutated virus also. Although we obtained a substantial amount of evidence that C/EBP enhanced the distal *TR-L1* promoter of LMP1, activation of the proximal *ED-L1* promoter was checked only by the reporter assays. We were not able to confirm this, because PCR primers that detect only the *ED-L1* promoter could not be designed.

Previous studies have repeatedly demonstrated that cytokines such as IL-4, IL-6, IL-10, and IL-21 mediate *LMP1* gene expression in the absence of the viral coactivator EBNA2, namely in type II latent cells such as B cells (10–12, 36), NK/T lymphomas (11), epithelial HeLa cells, and the NPC-derived cell line CNE2 (14). More amazingly, expression patterns of EBV proteins even in type I or III cells could be modulated by cytokines to resemble those in type II latency (10–12, 36). These reports all showed engagement of the JAK/STAT signaling pathway in the process of induction of *LMP1* expression. We suggest new information on the involvement of the C/EBP family, which has been implicated in various physiological phenomena, such as differentiation, inflammation, and cell growth. In terms of inflammation, C/EBP proteins have been implicated in induction of a number of cytokines (37, 38). For example, C/EBP plays a role in transcriptional induction of certain genes by IL-6 (39). IL-10 activates expression of C/EBP and thereby activates transcription of IL-6 in epithelial cells (40). Therefore, it is strongly suggested that cytokines activate the *LMP1* promoter through C/EBP, besides JAK/STAT signaling. In addition to cytokine-induced expression of LMP1, it seems likely that C/EBP contributes to produce LMP1 even in the absence of cytokines, because expression of *LMP1* in the AGS cell line with recombinant EBV mutated at the C/EBP binding site was notably more subdued than with the wild-type virus (Fig. 7, *A* and *B*).

To summarize, we could successfully identify as a new factor C/EBP as the transcriptional activator of the major oncogene of EBV, *LMP1*, and made an initial characterization of the molecular mechanisms of how *LMP1* expression is reinforced by the transcription factor in an EBNA2-independent manner. Because *LMP1* is the major oncogene of EBV, suppression of *LMP1* gene expression by inhibiting the C/EBP family may provide potential targets of therapeutic drugs for EBV-positive cancers, especially for type II cancers, such as NK/T lymphomas, NPC, and Hodgkin lymphomas. Search for small molecules that inhibit *LMP1* expression is already under way.

Acknowledgments—We thank Drs. W. Hammerschmidt, H. J. Delecluse, S. Tsuzuki, and S. W. Tsao for providing the EBV-BAC system, HEK293 cells, shRNA technology, and C666-1 cells. We also are grateful to Dr. N. Raab-Traub for materials used in the preliminary experiments. We also express our appreciation to N. Hotta and T. Gamano for technical assistance.

REFERENCES

1. Soni, V., Cahir-McFarland, E., and Kieff, E. (2007) *Adv. Exp. Med. Biol.* **597,** 173–187
2. Lam, N., and Sugden, B. (2003) *Cell. Signal.* **15,** 9–16
3. Shair, K. H., Bendt, K. M., Edwards, R. H., Bedford, E. C., Nielsen, J. N., and Raab-Traub, N. (2007) *PLoS Pathog.* **3,** e166
4. Kulwichit, W., Edwards, R. H., Davenport, E. M., Baskar, J. F., Godfrey, V., and Raab-Traub, N. (1998) *Proc. Natl. Acad. Sci. U.S.A.* **95,** 11963–11968
5. Johannsen, E., Koh, E., Mosialos, G., Tong, X., Kieff, E., and Grossman, S. R. (1995) *J. Virol.* **69,** 253–262
6. Laux, G., Adam, B., Strobl, L. J., and Moreau-Gachelin, F. (1994) *EMBO J.* **13,** 5624–5632
7. Grossman, S. R., Johannsen, E., Tong, X., Yalamanchili, R., and Kieff, E. (1994) *Proc. Natl. Acad. Sci. U.S.A.* **91,** 7568–7572
8. Harada, S., and Kieff, E. (1997) *J. Virol.* **71,** 6611–6618
9. Kis, L. L., Gerasimcik, N., Salamon, D., Persson, E. K., Nagy, N., Klein, G., Severinson, E., and Klein, E. (2011) *Blood* **117,** 165–174
10. Kis, L. L., Salamon, D., Persson, E. K., Nagy, N., Scheeren, F. A., Spits, H., Klein, G., and Klein, E. (2010) *Proc. Natl. Acad. Sci. U.S.A.* **107,** 872–877
11. Kis, L. L., Takahara, M., Nagy, N., Klein, G., and Klein, E. (2006) *Blood* **107,** 2928–2935
12. Konforte, D., Simard, N., and Paige, C. J. (2008) *Virology* **374,** 100–113
13. Chen, H., Lee, J. M., Zong, Y., Borowitz, M., Ng, M. H., Ambinder, R. F., and Hayward, S. D. (2001) *J. Virol.* **75,** 2929–2937
14. Chen, H., Hutt-Fletcher, L., Cao, L., and Hayward, S. D. (2003) *J. Virol.* **77,** 4139–4148
15. Sadler, R. H., and Raab-Traub, N. (1995) *J. Virol.* **69,** 4577–4581
16. Hsiao, J. R., Chang, K. C., Chen, C. W., Wu, S. Y., Su, I. J., Hsu, M. C., Jin, Y. T., Tsai, S. T., Takada, K., and Chang, Y. (2009) *Cancer Res.* **69,** 4461–4467
17. Sjöblom, A., Yang, W., Palmqvist, L., Jansson, A., and Rymo, L. (1998) *J. Virol.* **72,** 1365–1376
18. Tsai, C. N., Lee, C. M., Chien, C. K., Kuo, S. C., and Chang, Y. S. (1999) *Virology* **261,** 288–294
19. Ning, S., Hahn, A. M., Huye, L. E., and Pagano, J. S. (2003) *J. Virol.* **77,** 9359–9368
20. Maruo, S., Yang, L., and Takada, K. (2001) *J. Gen. Virol.* **82,** 2373–2383
21. Kanda, T., Yajima, M., Ahsan, N., Tanaka, M., and Takada, K. (2004)

J. Virol. **78,** 7004–7015
22. Murata, T., Hotta, N., Toyama, S., Nakayama, S., Chiba, S., Isomura, H., Ohshima, T., Kanda, T., and Tsurumi, T. (2010) *J. Biol. Chem.* **285,** 23925–23935
23. Murata, T., Sato, Y., Nakayama, S., Kudoh, A., Iwahori, S., Isomura, H., Tajima, M., Hishiki, T., Ohshima, T., Hijikata, M., Shimotohno, K., and Tsurumi, T. (2009) *J. Biol. Chem.* **284,** 8033–8041
24. Brummelkamp, T. R., Bernards, R., and Agami, R. (2002) *Cancer Cell* **2,** 243–247
25. Murata, T., Noda, C., Saito, S., Kawashima, D., Sugimoto, A., Isomura, H., Kanda, T., Yokoyama, K. K., and Tsurumi, T. (2011) *J. Biol. Chem.* **286,** 22007–22016
26. Delecluse, H. J., Hilsendegen, T., Pich, D., Zeidler, R., and Hammerschmidt, W. (1998) *Proc. Natl. Acad. Sci. U.S.A.* **95,** 8245–8250
27. Murata, T., Isomura, H., Yamashita, Y., Toyama, S., Sato, Y., Nakayama, S., Kudoh, A., Iwahori, S., Kanda, T., and Tsurumi, T. (2009) *Virology* **389,** 75–81
28. Ramji, D. P., and Foka, P. (2002) *Biochem. J.* **365,** 561–575
29. Osada, S., Yamamoto, H., Nishihara, T., and Imagawa, M. (1996) *J. Biol. Chem.* **271,** 3891–3896
30. Cooper, C., Henderson, A., Artandi, S., Avitahl, N., and Calame, K. (1995) *Nucleic Acids Res.* **23,** 4371–4377
31. Yoshiyama, H., Imai, S., Shimizu, N., and Takada, K. (1997) *J. Virol.* **71,** 5688–5691
32. Burda, P., Laslo, P., and Stopka, T. (2010) *Leukemia* **24,** 1249–1257
33. Gupta, P., Gurudutta, G. U., Saluja, D., and Tripathi, R. P. (2009) *J. Cell Mol. Med.* **13,** 4349–4363
34. Sugiyama, T., Uchida, C., Oda, T., Kitagawa, M., Hayashi, H., and Ichiyama, A. (2001) *FEBS Lett.* **508,** 16–22
35. Kilareski, E. M., Shah, S., Nonnemacher, M. R., and Wigdahl, B. (2009) *Retrovirology* **6,** 118
36. Kis, L. L., Takahara, M., Nagy, N., Klein, G., and Klein, E. (2006) *Immunol. Lett.* **104,** 83–88
37. Tsukada, J., Yoshida, Y., Kominato, Y., and Auron, P. E. (2011) *Cytokine* **54,** 6–19
38. Kalvakolanu, D. V., and Roy, S. K. (2005) *J. Interferon Cytokine Res.* **25,** 757–769
39. Kordula, T., and Travis, J. (1996) *Biochem. J.* **313,** 1019–1027
40. Robb, B. W., Hershko, D. D., Paxton, J. H., Luo, G. J., and Hasselgren, P. O. (2002) *Surgery* **132,** 226–231

THE JOURNAL OF BIOLOGICAL CHEMISTRY VOL. 286, NO. 25, pp. 22007–22016, June 24, 2011

Involvement of Jun Dimerization Protein 2 (JDP2) in the Maintenance of Epstein-Barr Virus Latency*[S]

Received for publication, November 2, 2010, and in revised form, April 17, 2011 Published, JBC Papers in Press, April 27, 2011, DOI 10.1074/jbc.M110.199836

Takayuki Murata[‡], Chieko Noda[‡], Shinichi Saito[‡], Daisuke Kawashima[‡], Atsuko Sugimoto[‡], Hiroki Isomura[‡], Teru Kanda[‡], Kazunari K. Yokoyama[§], and Tatsuya Tsurumi[‡1]

From the [‡]Division of Virology, Aichi Cancer Center Research Institute, 1-1, Kanokoden, Chikusa-ku, Nagoya 464-8681, Japan and the [§]Center of Excellence for Environmental Medicine, Cancer Center, Graduate Institute of Medicine, Kaohsiung Medical University, 807 Kaohsiung, Taiwan

Reactivation of the Epstein-Barr virus from latency is dependent on expression of the BZLF1 viral immediate-early protein. The *BZLF1* promoter (Zp) normally exhibits only low basal activity but is activated in response to chemical inducers such as 12-*O*-tetradecanoylphorbol-13-acetate and calcium ionophore. We found that Jun dimerization protein 2 (JDP2) plays a significant role in suppressing Zp activity. Reporter, EMSA, and ChIP assays of a Zp mutant virus revealed JDP2 association with Zp at the ZII *cis*-element, a binding site for CREB/ATF/AP-1. Suppression of Zp activity by JDP2 correlated with HDAC3 association and reduced levels of histone acetylation. Although introduction of point mutations into the ZII element of the viral genome did not increase the level of BZLF1 production, silencing of endogenous *JDP2* gene expression by RNA interference increased the levels of viral early gene products and viral DNA replication. These results indicate that JDP2 plays a role as a repressor of Zp and that its replacement by CREB/ATF/AP-1 at ZII is crucial to triggering reactivation from latency to lytic replication.

The Epstein-Barr virus (EBV)[2] is a human γ-herpesvirus that predominantly establishes latent infection in B lymphocytes. Only a small percentage of infected cells switch from the latent stage into the lytic cycle to produce progeny viruses. Although the mechanism of EBV reactivation *in vivo* is not fully understood, it is known to be elicited by treatment of latently infected B cells with chemical or biological reagents, such as 12-*O*-tetradecanoylphorbol 13-acetate (TPA), calcium ionophore, sodium butyrate, or anti-immunoglobulin, at least in cultured cells. Stimulation of the EBV lytic cascade by any of these leads to expression of two immediate-early genes, *BZLF1* and *BRLF1*. The BZLF1 protein is a transcriptional activator that shares structural similarities to basic leucine zipper (b-Zip) family transcriptional factors and acts as an oriLyt binding protein essential for lytic viral DNA replication. BZLF1 expression alone can trigger the entire reactivation cascade (1–3).

Expression of the *BZLF1* gene is tightly controlled at the transcriptional level. The *BZLF1* promoter (Zp) normally exhibits low basal activity and is activated in response to TPA or the other reagents described above. The minimal sequence of Zp necessary for activation by the inducers is 233 bp in length (4). The region harbors at least three types of *cis* regulatory elements, referred to as ZI, ZII, and ZIII. Four copies of the ZI element (ZIA–D) are distributed within the minimal Zp. The myocyte enhancer factor 2D binds to ZIA, ZIB, and ZID (5), whereas Sp1 or Sp3 can bind to ZIA, ZIC, and ZID (6). A single ZII element is located near TATA, sharing homology with binding sites for the cyclic AMP-response element-binding protein (CREB), activating transcription factor (ATF), and activator protein-1 (AP-1) family transcriptional factors such as JunB and JunD (7, 8). Two copies of the ZIII element (ZIII-A and -B) bind to the BZLF1 protein. Previous studies have demonstrated that both ZI and ZII elements are necessary for the initial activation of the promoter by TPA/ionophore or anti-surface immunoglobulin IgG (2). Then, the expressed BZLF1 protein further activates Zp by binding to ZIIIA and -B (9). BZLF1 also activates transcription of other viral immediate-early or early genes and enhances the lytic infection cycle of the virus.

The Jun dimerization protein 2 (JDP2) was initially identified as a binding partner of the AP-1 transcription factor, c-Jun (10). It appears ubiquitously expressed and is involved in a variety of biological phenomena, such as cell differentiation (11–14), apoptosis (15, 16), and tumorigenesis (17–22). It can dimerize, through its b-Zip motif, with itself or other b-Zip proteins, such as c-Jun, JunB, JunD, or ATF-2 (10, 11, 23), and function as a general repressor of, at least, AP-1, cAMP-response element, and TPA responsive element-dependent transcription (10, 23). It has been reported that JDP2 recruits histone deacetylase 3 (HDAC3) to the promoters of target genes and inhibits histone acetyltransferase activity, thereby suppressing transcriptional activity (14, 24). Depending on the context and cell type, however, it can alternatively act as a transcriptional activator (25, 26).

In the present study, we obtained evidence that JDP2 suppresses Zp mainly through interaction with the ZII *cis*-element.

* This work was supported by Grants-in-Aid for Scientific Research from the Ministry of Education, Science, Sports, Culture and Technology of Japan 20390137 and 21022055 (to T. T.) and 20790362 and 22790448 (to T. M.), and grants from the Uehara Memorial Research Fund (to T. T.) and the Japan Leukaemia Research Fund (to T. M.).

[S] The on-line version of this article (available at http://www.jbc.org) contains supplemental Figs. S1–S4.

[1] To whom correspondence should be addressed. Tel./Fax: 81-52-764-2979; E-mail: ttsurumi@aichi-cc.jp.

[2] The abbreviations used are: EBV, Epstein-Barr virus; Zp, *BZLF1* promoter; JDP2, Jun dimerization protein 2; CREB, cyclic AMP-responsive element-binding protein; AP-1, activator protein-1; ATF, activating transcription factor; XBP1(s), spliced form of X-box binding protein 1; TPA, 12-*O*-tetradecanoylphorbol 13-acetate; b-Zip, basic leucine zipper; CMV, cytomegalovirus; HDAC, histone deacetylase; KO, knock-out.

The lytic life cycle of the virus was found to be significantly enhanced by silencing of endogenous JDP2 expression. We also found that JDP2 supported recruitment of HDAC3 to Zp. These results indicate that JDP2 plays critical roles in regulation of the latent-lytic switch in EBV infection.

EXPERIMENTAL PROCEDURES

Cell Culture and Antibodies—HEK293T and EBV-BAC 293 cells were maintained in Dulbecco's modified Eagle's medium (Invitrogen) supplemented with 10% fetal bovine serum. HEK293 cells with *BZLF1* knock-out (BZLF1KO) EBV were prepared as described previously (27). B95-8 cells were cultured in RPMI1640 medium supplemented with 10% fetal bovine serum. TPA and A23187 were added to induce lytic replication of EBV. Anti-human IgG (Dako Cytomation, A0423) was used for viral lytic induction in Akata cells, which were maintained in RPMI1640 medium supplemented with 10% fetal bovine serum. Anti-JDP2 rabbit antiserum was a gift from Dr. A. Aronheim (The Rappaport Family Institute for Research in the Medical Sciences, Technion-Israel Institute of Technology, Israel). Anti-GAPDH, -HDAC3, and acetylated histone H3K9 antibodies were from Ambion, Abcam, and Active Motif, respectively. Both mouse and rabbit anti-FLAG antibodies were from Sigma. Rabbit anti-BZLF1, -BMRF1, -BALF2, and -BALF5 antibodies were as reported previously (28). Horseradish peroxidase-linked goat antibodies to mouse or rabbit IgG were from Amersham Biosciences.

Plasmid Construction—The expression vector for BZLF1 (pcDNABZLF1), b-Zip deletion form of BZLF1 (pcDNAdBZLF1), the reporter plasmid pZp-luc and its derivatives, pZpmZII-luc, pZpmZIII-luc, and pZpmZII+III-luc, were constructed as described previously (29). An expression vector for FLAG-tagged BZLF1 (pcDNAFlagBZLF1) was prepared by inserting the *BZLF1* cDNA sequence into the EcoRI/XbaI site of pcDNAFLAG (29). FLAG-tagged expression vectors for CREB (30) and c-Jun (31) were as reported previously. For pcDNAFlagXBP1(s), the cDNA sequence for XBP1(s) (32) was amplified using the following primers: 5′-CATGGACTACAAGGACGACGATGACAAGATGGTGGTGGTGGCAGCCGC-3′ and 5′-CTTAGACACTAATCAGCTGGG-3′. Underlined nucleotides indicate the FLAG epitope. The amplified DNA was phosphorylated by polynucleotide kinase and then inserted into the EcoRV site of the pcDNA3 vector. The pCMV-RL reporter plasmid was obtained commercially (Stratagene). pCMV-FlagJDP2 was made by inserting human *JDP2* cDNA into the NotI site of pCMV_S-FLAG (RIKEN, RDB 5956). A deletion mutant at the b-Zip domain of *JDP2* was generated by PCR using primers 5′-CGCCCCACCTGCATCGTCC-3′ and 5′-TCGCTCCTCTTCCTCATCTAG-3′.

Transfection, Luciferase Assay, and Immunoblotting—Plasmid DNA was transfected into HEK293T or EBV-BAC 293 cells using Lipofectamine 2000 reagent (Invitrogen). The total amounts of plasmid DNA were standardized by addition of an empty vector. Proteins were extracted from cells with the lysis buffer supplied in a Dual-Luciferase Reporter Assay System (Promega) kit and luciferase activities were measured using the kit. Akata cells were electronically transfected using a Microporator (Digital Bio). Protein samples were subjected to SDS-PAGE, followed by immunoblotting with the indicated antibodies as described previously (29).

Electromobility Shift Assay (EMSA)—FLAG-tagged JDP2 proteins were produced using the TnT Quick Coupled Transcription/Translation System (Promega) according to the manufacturer's instructions. The probe was prepared by 3′-end labeling using Klenow fragment (TOYOBO) and [^{32}P]dATP (Institute of Isotopes Co., Hungary). Unincorporated deoxynucleotide triphosphates were removed with Chromaspin-10 columns (Clontech). The *in vitro* translated protein and labeled DNA sequences were incubated in the EMSA binding buffer (20 mM Tris-HCl, pH 7.6, 0.5 mM EDTA, 0.5 mM dithiothreitol, 10% glycerol, 30 mM KCl, 3 mM $MgCl_2$, 0.5 mg/ml of poly(dI-dC)) at room temperature for 30 min. The samples were then separated in a 4% non-denaturing polyacrylamide gel in 0.5× TBE buffer and the radioactivities were visualized by using BAS2500 system (Fuji Film). The sequences of oligonucleotide probes were as follows: ZII, 5′-CCCAAACCATGACATCACAGAG-3′ and 5′-CTCCTCTGTGATGTCATGGTTTGGG-3′; ZIIIA, 5′-AACTATGCATGAGCCACAGG-3′ and 5′-ATGCCTGTGGCTCATGCATAGTT-3′; ZIIIB, 5′-CACAGGCATTGCTAATGT-3′ and 5′-GAGGTACATTAGCAATGCCTGTG-3′.

siRNA, Exogenous Expression, and RT-PCR—Duplexes of a 21-nucleotide small interfering RNA (siRNA) specific to *JDP2* mRNA, including two nucleotides of deoxythymidine at the 3′ end, were synthesized and annealed (Gene Design, Inc). The sense and antisense sequences of the duplex were 5′-GUGAGCUAGAUGAGGAAGAdTdT-3′ and 5′-UCUUCCUCAUCUAGCUCACdTdT-3′ (si-JDP2.1) and 5′-GCACAUACUCACCGAAUGUdTdT-3′ and 5′-ACAUUCGGUGAGUAUGUGCdTdT-3′ (si-JDP2.2), respectively. The control siRNA sequences were 5′-GCAGAGCUGGUUUAGUGAAdTdT-3′ and 5′-UUCACUAAACCAGCUCUGCdTdT-3′. Akata or B95-8 cells (1×10^5) were transfected with 50 pmol of the duplex RNA or with 300 ng of expression plasmid per well of a 24-well plate, using a Microporator (Digital Bio). 24 or 48 h after transfection, TPA plus A23187, or anti-IgG was added to induce lytic replication and incubated for another 12 or 24 h. Cells were then harvested for quantification by real time RT-PCR using the One-Step SYBR PrimeScript RT-PCR Kit II (TaKaRa). PCR was performed in 10 μl of solution containing 0.2 μM primers, 0.2 μl of ROX Dye, and the sample RNA in 1× One-Step SYBR RT-PCR buffer. Intensity of ROX Dye was used to compensate the volume fluctuations among the tubes. PCR included 5 min at 42 °C, 10 s at 95 °C, and 40 cycles at 95 °C for 5 s followed by 40 s at 60 °C. Immediately after the RT-PCR, we carried out dissociation curve analysis and confirmed the specificity of each PCR product. An arbitrary RNA was set to 1.0 and a standard curve was constructed using serial dilutions of RNA from the RNA set to 1.0. The amount of mRNA was quantitated based on the standard curve. Real time PCR with RNA polII primers was also performed to serve as an internal control for input RNA. Primers used for the real time RT-PCR were as follows: for *JDP2* mRNA, 5′-CTGTGGAGGAGCTGAAATAC-3′ and 5′-ATCTAGCTCACTTTTCACGG-3′, for *BZLF1* mRNA, 5′-AACAGCCAGAATCGCTGGAG-3′ and 5′-GGCACATCTGCTTCAACAGG-3′, for *RNApolII* 5′-GCACCAC-

GTCCAATGACAT-3′ and 5′-GTGCGGCTGCTTCCATAA-3′. Viral DNA levels were assayed by dot-blot hybridization as described previously (28, 33).

Genetic Manipulation of EBV-BAC DNA and Cloning of HEK293 Cells with EBV-BAC—EBV-BAC DNA was provided by W. Hammerschmidt (34). Homologous recombination was carried out in *Escherichia coli* as described previously (28).

To prepare an mZII mutant of EBV-BAC, a transfer DNA fragment for the first recombination was generated by PCR using PpsL-neo (Gene Bridges) as the template, with the following primers: 5′-AGCCACAGGCATTGCTAATGTACCTCA-TAGACACACCTAAATTTAGCACGTCCCAAACCAGGC-CTGGTGATGATGGCGGGATC-3′ and 5′-GAGTTACCT-GTCTAACATCTCCCCTTTAAAGCCAAGGCACCAGCC-TCCTCTGTGATGTCATCAGAAGAACTCGTCAAGAAG-G-3′. After the recombination, kanamycin-resistant colonies were selected and checked to make intermediate DNA. The NeoSt+ cassette in the intermediate DNA was then replaced using the next transfer vector DNA, containing a mutation in the ZII *cis*-element of Zp. The transfer vector was made by PCR using pZpmZII-luc as the template with the following primers: 5′-ACCAGCTTATTTTAGACACTTC-3′ and 5′-GTTTGG-GTCCATCATCTTCAG-3′. Streptomycin-resistant colonies were cloned and checked to make the EBV-BAC mZII mutant. Likewise, a revertant of the mZII mutant (EBV-BAC mZII/R) was created by re-insertion of the NeoSt+ cassette and its rescue using a wild-type *BZLF1* promoter sequence.

Electroporation of *E. coli* was performed using Gene Pulser III (Bio-Rad) and purification of EBV-BAC DNA was achieved with NucleoBond Bac100 (Macherey-Nagel). Recombination was confirmed with PCR products of the Zp region, electrophoresis of the BamHI-digested viral genome, and sequencing analysis.

EBV-BAC DNA was transfected into HEK293 cells using Lipofectamine 2000 reagent (Invitrogen), which were then cultured on 10-cm dishes with 100–150 μg/ml of hygromycin B for 10–15 days for cloning of GFP-positive cell colonies as described previously (28). Briefly, for each recombinant virus, we picked up more than 10 hygromycin-resistant, GFP-positive cell colonies to obtain at least 3 typical clones exhibiting minimal spontaneous expression of viral lytic proteins and significant induction of these upon BZLF1 transfection.

ChIP Assays—ChIP assays were performed essentially as described (Upstate Biotechnology, Inc.) with formaldehyde cross-linked chromatin from 1×10^6 cells for each reaction. Cells were lysed, and chromatin was sonicated to obtain DNA fragments with an average length of 300 bp. Following centrifugation, the chromatin was diluted 10-fold with ChIP dilution buffer, and precleared with protein A-agarose beads containing salmon sperm DNA (Upstate). Anti-FLAG antibody or normal rabbit IgG was added to the sample and incubation proceeded overnight with rotation. Immune complexes were then collected by addition of protein A-agarose beads and DNA was purified using a QIAquick PCR Purification Kit (Qiagen) after uncoupling of the cross-linking and proteinase K digestion. The recovered DNA was amplified by PCR using primers specific for Zp: 5′-TAGCCTCGAGGCCATGCATATTTCAACTGG-3′, 5′-GCCAAGCTTCAAGGTGCAATGTTTAGTGAG-3′, and for the EBNA1 open reading frame: 5′-GTCATCATCAT-CCGGGTCTC-3′ and 5′-TTCGGGTTGGAACCTCCTTG-3′. The PCR products were then analyzed by agarose gel electrophoresis and visualized with ethidium bromide. The samples were also subjected to real time PCR for quantification of DNA sequences using the same primers and SYBR Premix Ex TaqII (TaKaRa). Real time PCR was performed in 10 μl of solution containing 0.2 μM primers, 0.2 μl of ROX Dye, and the sample DNA in 1× One-Step SYBR RT-PCR buffer. Intensity of ROX Dye was used to compensate the volume fluctuations among the tubes. PCR included 10 s at 95 °C and 40 cycles at 95 °C for 5 s followed by 45 s at 60 °C. Immediately after the PCR, we carried out dissociation curve analysis and confirmed the specificity of each PCR product. An arbitrary DNA was set to 1.0 and a standard curve was constructed using serial dilutions of DNA from the DNA set to 1.0. The amount of DNA was quantitated based on the standard curve.

Immunoprecipitation Assay—For immunoprecipitation to detect the association between JDP2 and HDAC3, cells were lysed in Nonidet P-40 buffer (10 mM Tris-HCl, pH 7.8, 100 mM NaCl, 1 mM EDTA, 0.2% Nonidet P-40, and protease inhibitor mixture). After sonication and centrifugation, lysates were precleared with protein G-Sepharose, then mixed with anti-FLAG antibody and protein G-Sepharose for 4 h. The resin was washed 5 times with the same buffer and then samples were subjected to SDS-PAGE followed by immunoblotting with anti-JDP2 or FLAG antibody.

Data Analysis and Statistics—Data are presented as mean ± S.D. Statistical analysis was carried out using Student's *t* test and values considered significantly different when $p < 0.05$.

RESULTS

JDP2 Represses Transcription from EBV Zp—Because JDP2 represses transcriptional activation of reporter constructs containing cAMP-response element or TPA-responsive elements (23), we hypothesized that JDP2 might regulate the *BZLF1* transcription and thereby affect EBV reactivation. To investigate this possibility, we first carried out reporter gene assays. Co-transfection of the JDP2 expression vector clearly repressed reporter gene expression from pZp-luc, in the presence or absence of BZLF1 (data not shown). In this reporter assay, however, we co-transfected pCMV-RL, a *Renilla* luciferase reporter driven by the CMV immediate early promoter at the same time, and this reporter strongly responded negatively, regardless of BZLF1 (data not shown). This result pointed to a possibility that ectopic overexpression of JDP2 suppresses the CMV immediate-early promoter, as well as *BZLF1* promoter and that this system is not suitable for analyses of specific effects of JDP2 on the Zp.

Therefore, we adopted siRNA technology, using synthetic oligonucleotides that form duplex RNA encoding partial nucleotides from *JDP2*. As shown in Fig. 1*A*, cotransfection with the BZLF1 expression vector (Z) caused increased Zp activity, due to its autoactivation ability. Treatment with an siRNA (si-JDP2.1) significantly elevated the transcriptional activity from the wild-type *BZLF1* promoter (pZp-luc(wt)), either in the presence or absence of BZLF1 (Fig. 1*A*). Another siRNA (si-JDP2.2) also resulted in increased Zp activity (Fig. 1*A*). Interest-

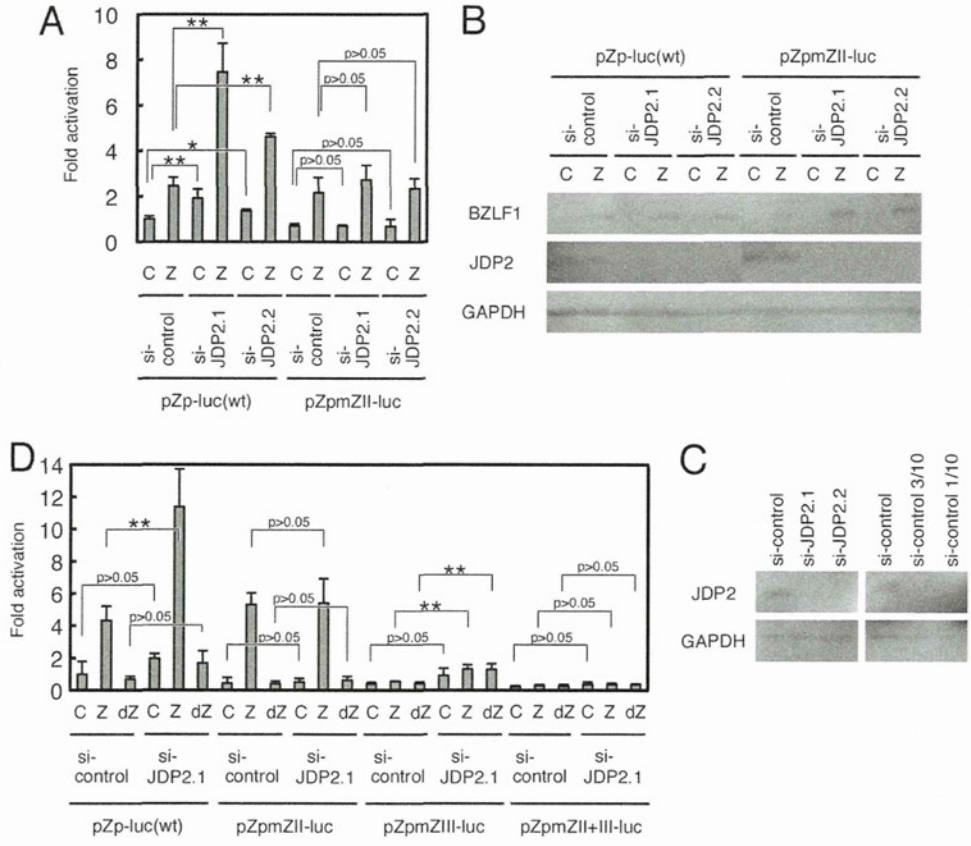

FIGURE 1. **Knockdown of endogenous JDP2 enhances transcription from Zp.** *A–C*, HEK293T cells were transfected with duplexes of a 21-nucleotide siRNA against JDP2 (*si-JDP2.1* or *si-JDP2.2*) or a control (*si-control*) siRNA, together with 10 ng of pZp-luc or its derivative, pZpmZII-luc, and 1 ng of pCMV-RL with 10 ng of empty vector (*C*) or pcDNABZLF1 (*Z*). Luciferase assays (*A*) were carried out 36 h after the transfection, as described under "Experimental Procedures." Each *bar* illustrates the mean ± S.D. of three independent transfections. The luciferase activities are shown as fold-activation of that for pZp-luc(wt), with the si-control and empty vector (*leftmost bar*). *B*, protein levels of BZLF1, JDP2, and GAPDH in the assay were examined by immunoblotting. *C*, JDP2 levels in samples transfected with si-JDP2.1 or si-JDP2.2 in the assay were compared with 100, 30, or 10% of the control. *D*, HEK293T cells were transfected with siRNA against JDP2 (si-JDP2.1) or a control (si-control) siRNA, together with 10 ng of pZp-luc or its derivatives and 1 ng of pCMV-RL with 10 ng of empty vector (*C*), pcDNABZLF1 (*Z*), or pcDNAdBZLF1 (*dZ*). pcDNAdBZLF1 (*dZ*) expresses BZLF1 protein lacking the b-Zip domain. Luciferase assays were carried out 36 h after the transfection, as described under "Experimental Procedures." * or ** indicates $p < 0.05$ or $p < 0.02$, respectively.

ingly, silencing of endogenous *JDP2* did not affect the CMV promoter as monitored by the reporter assay (data not shown). On the other hand, when the ZII motif in the Zp was mutated (pZpmZII-luc), a significant response to JDP2 knockdown was not observed (Fig. 1*A*). Knockdown of the JDP2 protein was checked by immunoblotting (Fig. 1*B*). Real time PCR analysis indicated that si-JDP2.1 and si-JDP2.2 reduced the *JDP2* mRNA levels down to 23 and 43% of the control (data not shown). We also examined that levels of the BZLF1 protein were relatively constant (Fig. 1*B*). To quantify the levels of JDP2 knockdown, protein samples transfected with si-JDP2.1 or si-JDP2.2 were compared with those from control cells after serial dilution (Fig. 1*C*). Either of the siRNAs reduced the JDP2 protein levels to ~30% or less in HEK293T cells. These results suggest that JDP2 inhibit Zp through the ZII *cis*-element, which is known to be bound by cellular transcription factors such as CREB/ATF/AP-1.

The site-directed mutation of the ZIII element, which prevents BZLF1 binding, failed to respond to ectopic expression of the BZLF1 protein (Fig. 1*D*) as expected, but its promoter activity was increased by si-JDP2 treatment (Fig. 1*D*, pZpmZIII-luc). Although *p* values indicate that JDP2 knockdown did not always cause statistically significant augmentation of wild-type or mZIII promoters, these results imply that JDP2 decreases Zp activity and that the suppressive effect of JDP2 is mediated through the ZII motif, but not through the ZIII of *BZLF1* promoter.

JDP2 Binds to ZII Motif in Vitro—Reporter assays suggested JDP2 association with the ZII element, but not with the ZIII elements. To confirm the binding of JDP2 to the ZII *cis*-element, EMSA was carried out in Fig. 2. Addition of FLAG-tagged JDP2 produced a specific band of JDP2-ZII complex (Fig. 2, *lane 2*). Excess amounts of unlabeled ZII competitor clearly reduced the intensities of the shifted band (*lane 3*), whereas the cold ZIIIA or ZIIIB did not (*lanes 4* or *5*, respectively). When JDP2 lacking b-Zip domain (FlagdJDP2, *lane 8*) was used instead of wild-type FlagJDP2 (*lane 7*), no obvious shift was detected (Fig. 2, *right*). Supershift analysis with anti-FLAG antibody demonstrated that the band actually contained FLAG-tagged JDP2 protein (*lane 9*). Therefore, JDP2 binds to ZII, but not to the ZIIIA or ZIIIB *cis*-elements of Zp.

Association of JDP2 with the BZLF1 Promoter in Vivo—To further verify the reporter assays and EMSA results, we performed ChIP analysis using cells containing wild-type or *BZLF1* knock-out (BZLF1KO) EBV-BAC (27). We used the BZLF1KO mutant strain, to exclude the possibility that BZLF1 is involved

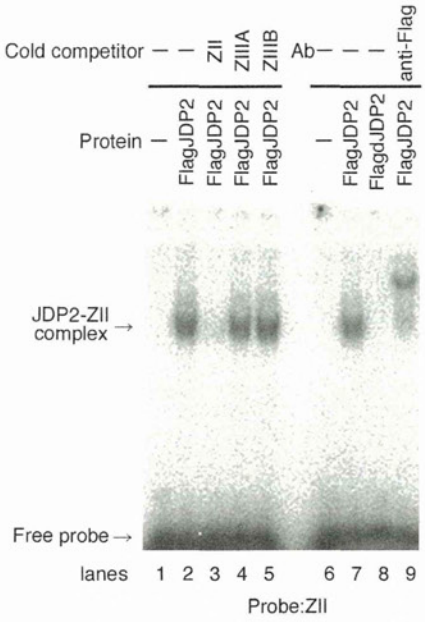

FIGURE 2. **JDP2 binds to ZII motif in the *BZLF1* promoter *in vitro*.** EMSA was carried out as described under "Experimental Procedures." FLAG-tagged wild-type JDP2 protein (*FlagJDP2*) or JDP2 protein lacking b-Zip domain (*FlagdJDP2, lane 8*) was produced *in vitro* and incubated with ^{32}P-labeled probe and excessive amounts of cold competitors (ZII (*lane 3*), ZIIIA (*lane 4*), and ZIIIB (*lane 5*)). Supershift analysis was performed using mouse anti-FLAG monoclonal antibody (*lane 9*). The samples were then separated in a 4% polyacrylamide gel and analyzed with Fuji Image Analyzer BAS2500.

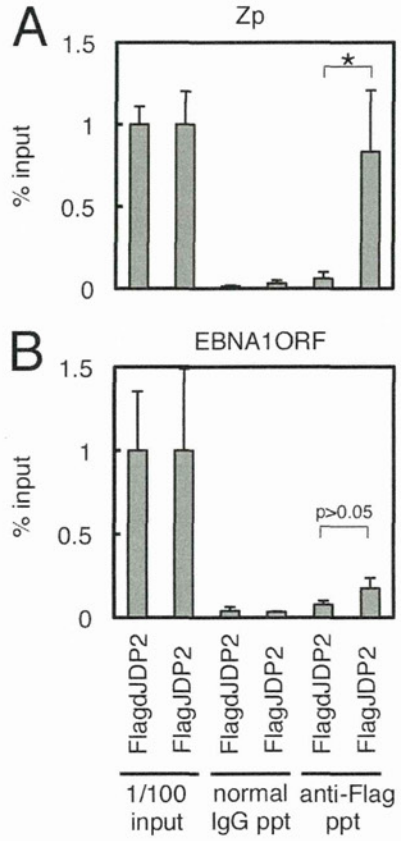

FIGURE 3. **Association of JDP2 with the *BZLF1* promoter.** HEK293 cells with *BZLF1* knock-out (BZLF1KO) EBV-BAC DNA were transfected with the FlagJDP2 expression vector (*FlagJDP2*), or the FlagJDP2 expression vector with a deletion in the b-Zip domain (*FlagdJDP2*). After 24 h, ChIP experiments were carried out using cross-linked DNA-protein complexes from the cells, precipitated using normal IgG or anti-FLAG antibody, followed by DNA extraction and PCR to detect the Zp (*A*). A fragment for the EBNA1 open reading frame was also detected as a negative control (*B*). * indicates $p < 0.05$.

in the association between JDP2 and the *BZLF1* promoter. The *BZLF1* promoter region was obviously co-precipitated with FLAG-tagged JDP2 (supplemental Fig. S1*A*), either in wild-type or BZLF1KO. A primer set for the EBNA1 coding region was included as a negative control to prove that the signal for the Zp was specific. This experiment of BZLF1KO was repeated and quantified in Fig. 3. With wild-type JDP2, the Zp was significantly concentrated when compared to the level of dJDP2 (*Fig. 3A*). Thus, the association proved to be intact, indicating that BZLF1 is not needed for JDP2 binding to the *BZLF1* promoter sequence.

Because the above documented results indicated JDP2 acts to suppress the *BZLF1* promoter by binding to the ZII *cis*-element, we generated recombinant EBV with a point mutation in the ZII element (Fig. 4*A*). To this end, we first replaced the ZII element with a marker cassette (NeoSt+), and then exchanged this with the mutated ZII sequence, to prepare EBV-BAC mZII. The mutated ZII sequence of the EBV was again swapped with a NeoSt+ cassette, followed by replacement with the wild-type sequence, to generate a revertant strain, EBV-BAC mZII/R. Sequencing analysis confirmed that the EBV-BAC mZII DNA had the same mutation as the pZpmZII-luc vector (Fig. 1), and that the EBV-BAC mZII/R had the same sequence as the wild-type virus, as intended. Integrity of the BAC DNA was checked by BamHI digestion followed by electrophoresis to confirm that the recombinant viruses did not carry obvious deletions or insertions (Fig. 4*B*). The BamHI-Z fragment was too short to be clearly detected.

Recombinant EBV-BAC DNA was introduced into HEK293 cells, followed by hygromycin selection, to establish cell lines in which multiple copies were maintained as an episome. More than 10 cell colonies from each recombinant virus were obtained and viral protein expression levels were examined. Fig. 4*C* shows immunoblotting data for typical cells. When the BZLF1 expression vector was transfected, the cells all responded and expressed viral genes, as expected. In the absence of BZLF1, however, levels of the viral genes in EBV-BAC mZII cells were noticeably lower than those in wild-type or revertant cells. Thus, introduction of point mutations into the ZII element of the viral genome did not increase BZLF1 production. We speculate that the suppressive JDP2 does bind to the ZII element in the latent phase but that its negative effect is counteracted by powerful stimulatory effects of other transcriptional factors, such as CREB/ATF/AP-1 family proteins. We here first demonstrated the significance of the ZII element in the context of the viral genome.

Although effects of JDP2 on *BZLF1* promoter activation were not observed in recombinant viruses, the ZII-mutant and its revertant viruses could still be used for binding assays. Supplemental Fig. S1*B* shows ChIP results. JDP2 was recruited to the *BZLF1* promoter in cells with the wild-type and revertant viruses, but this was impaired in cells with the mZII virus. Additionally, JDP2 with deletion in the b-Zip domain of the protein failed to target the *BZLF1* promoter (supplemental Fig. S1*B*, *right panels*). Taken together, the results indicate that JDP2 is

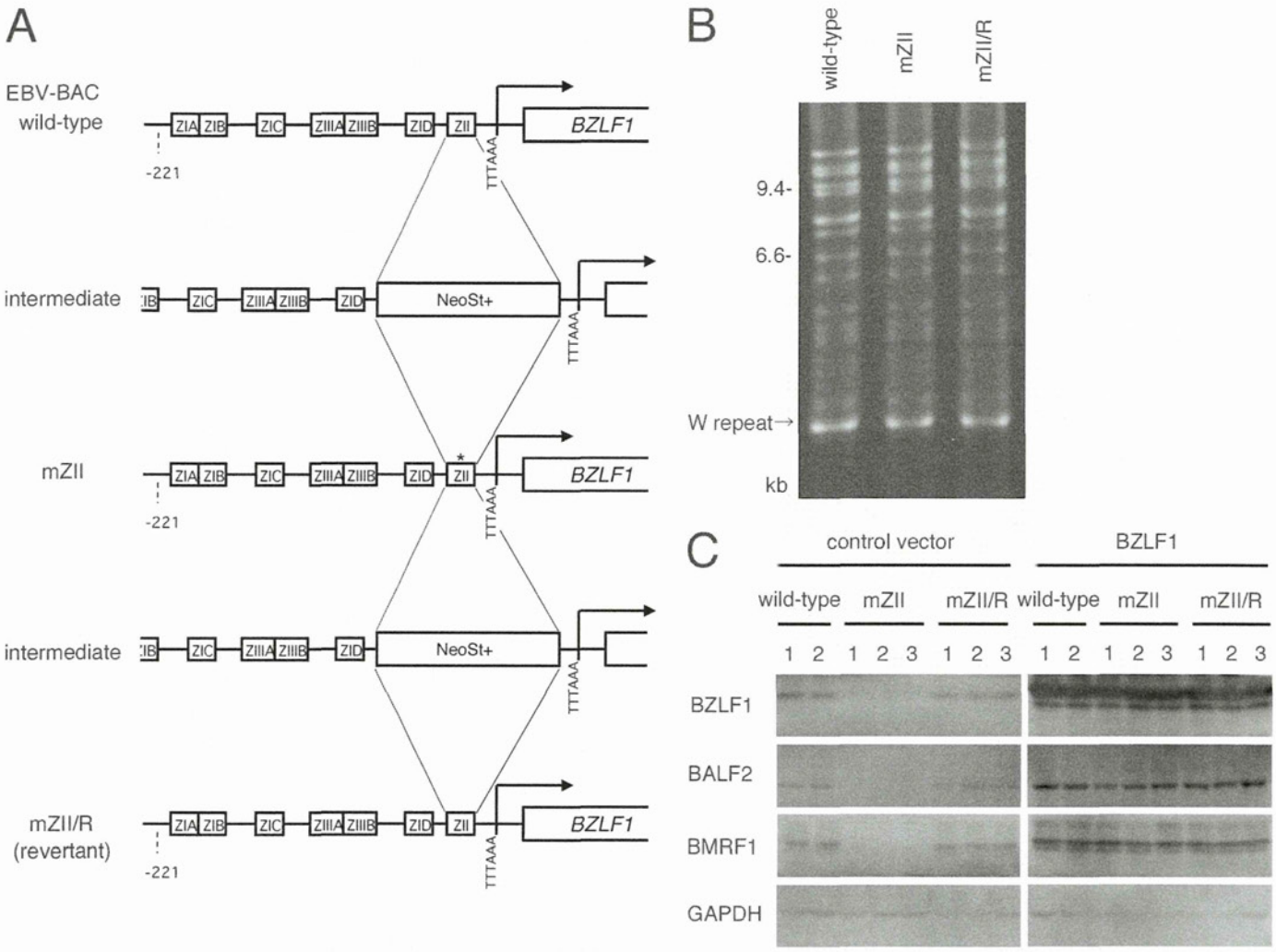

FIGURE 4. **Construction of recombinant EBV featuring point mutation in the ZII *cis*-element of the *BZLF1* promoter.** *A*, schematic arrangement of the recombination of the EBV genome using the tandemly arranged neomycin resistance and streptomycin sensitivity genes (*NeoSt*+). The ZII element of the B95-8 genome was first replaced with the NeoSt+ cassette, which was then replaced with a point-mutated ZII sequence (*asterisk*) to construct EBV-BAC mZII. The mutated ZII sequence was replaced again with the NeoSt+ marker cassette and swapped with the wild-type ZII sequence to prepare the revertant clone, EBV-BAC mZII/R. *B*, electrophoresis of the recombinant viruses. The recombinant EBV genomes were digested with BamHI and separated in an agarose gel. *C*, expression of viral proteins from the recombinant viruses. The recombinant EBV-BAC DNAs were introduced into HEK293 cells, followed by hygromycin selection. Resultant cell clones were tested for protein viral expression. The indicated clones of cells were transfected with the BZLF1 expression vector (BZLF1) or its empty control vector (control vector). After 48 h, cell proteins were harvested, and immunoblotting was performed using anti-BZLF1, -BALF2, -BMRF1, and -GAPDH antibodies.

recruited to the *BZLF1* promoter and binds to the ZII element through its b-Zip domain.

Because JDP2 and CREB, ATF, and AP-1 all bind to the ZII *cis*-element of the *BZLF1* promoter, we examined whether JDP2 could competitively block the binding of these b-Zip proteins (supplemental Fig. S2). HEK293 cells harboring wild-type EBV-BAC were transfected with siRNA against JDP2 or its control siRNA, together with or without the expression vector for FLAG-tagged -BZLF1, -CREB, and -c-Jun. We used the viral b-Zip protein BZLF1 as a control, which associates with the ZIII element of the *BZLF1* promoter (9). As expected, FLAG-BZLF1 bound to Zp, and cotransfection of the JDP2 siRNA did not alter the binding efficiency to the promoter (supplemental Fig. S2, *left panels*). On the other hand, binding was lower with control siRNA, and si-JDP2 treatment significantly increased the association of FLAG-tagged CREB and c-Jun with the promoter, compared with the si-control results (supplemental Fig. S2, *left panels*). Because a spliced form of X-box binding protein 1 (XBP1(s)) also reportedly targets the ZII element of Zp (35), we also tested for association. We could observe XBP1(s) binding to the Zp to be increased by si-JDP2 treatment, although this was not obvious in control-si experiments.

The competitive nature of JDP2 with CREB was reconfirmed and quantified in Fig. 5. When JDP2 was knocked down, FLAG-tagged CREB association with the Zp was significantly higher than that with the control siRNA (Fig. 5*A*). Immunoblotting data indicated the expression level of FLAG-CREB was not affected by si-JDP2 (Fig. 5*C*). These data indicate that JDP2 inhibits transcriptional activity of Zp by competitively occupying the ZII binding site.

Role of JDP2 in EBV Reactivation from Latency—To examine the role of JDP2 in EBV reactivation from latency under physiological conditions, B95-8 cells, latently infected with

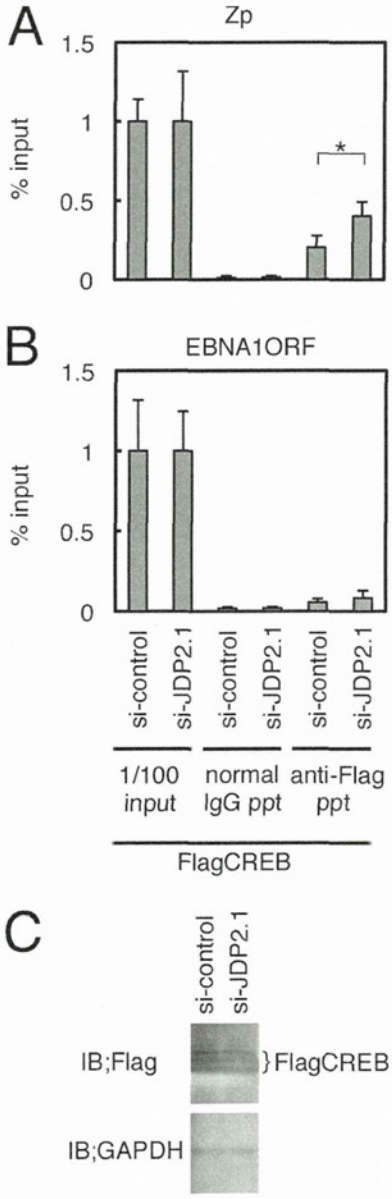

FIGURE 5. **Competitive binding of JDP2 with other b-Zip transcription factors.** HEK293 cells with wild-type EBV-BAC DNA were transfected with the siRNA against JDP2 (*si-JDP2.1*) or the control (*si-control*), together with FLAG-tagged expression vectors for CREB. After 36 h, ChIP experiments were carried out using cross-linked DNA-protein complexes from the cells, precipitated using normal IgG or anti-FLAG antibody, followed by DNA extraction and PCR to detect the Zp (*A*). A fragment for the EBNA1 open reading frame was also detected as a negative control (*B*). Levels of FLAG-tagged CREB protein were examined by immunoblotting (*IB*) (*C*). * indicates $p < 0.05$.

EBV, were treated with the siRNAs against JDP2. As shown in Fig. 6*B*, 73 or 49% suppression of the levels of *JDP2* mRNA resulted by si-JDP2.1 or si-JDP2. Although the knockdown of *JDP2* mRNA might not be perfect, it did reduce JDP2 protein levels (supplemental Fig. S3). JDP2 knockdown, in the absence of chemical lytic induction, augmented *BZLF1* levels 3.6- or 3.4-fold by si-JDP2.1 or si-JDP2.2, respectively (Fig. 6*A*), and the augmentation by si-JDP2.2, especially, was statistically significant. Treatment of TPA and A23187, a calcium ionophore, caused overall induction of the *BZLF1* gene, and si-JDP2.1 significantly induced *BZLF1* mRNA levels (Fig. 6*A*). A similar increase was also observed by si-JDP2.2 (Fig. 6*A*).

We then examined whether silencing of JDP2 influence viral lytic replication of another cell line (supplemental Fig. S4). Akata cells featuring latent infection were treated with the siRNA against JDP2. The levels of BZLF1 protein and early proteins, such as BMRF1, BALF5, and BALF2, were also enhanced, especially when treatment was combined with exposure to anti-IgG (supplemental Fig. S4).

To further confirm the role of JDP2, the effect of exogenous overexpression of JDP2 was monitored in B95-8 (Fig. 6, *C* and *D*) or HEK293 (Fig. 6, *E* and *F*) cells latently infected with EBV. Electroporation of FLAG-tagged JDP2 expression vector (FlagJDP2) or its deletion mutant (FlagdJDP2) elicited *JDP2* mRNA levels up to approximately 1,000-fold or more (Fig. 6, *D* and *F*). Expression of the dJDP2 mutant served as a negative control, as it lacks its b-Zip domain, and thus is not functional. In B95-8 cells, *BZLF1* mRNA levels were reduced significantly to about 50% by JDP2 overexpression with TPA and ionophore (Fig. 6*C*). Importantly, *BZLF1* expression patterns in HEK293 EBV/BAC cells with wild-type or the revertant strain (mZII/R) responded in similar ways (Fig. 6*E*) to JDP2 overexpression, whereas the *BZLF1* mRNA levels were not significantly affected by the overexpression in cells with the mZII mutant virus (Fig. 6*E*). These experiments strongly suggest that JDP2 suppresses *BZLF1* expression through the ZII motif in the promoter upon reactivation from latency.

JDP2 Mediates HDAC3 Recruitment to the BZLF1 Promoter—It has been reported that JDP2 recruits HDAC3 to the promoter of target genes and inhibits histone acetyltransferase activity, thereby suppressing transcriptional activity (14, 24). As exhibited previously, exogenously expressed FLAG-tagged JDP2 was able to associate with Zp (Fig. 7*A*, *left*), whereas its b-Zip deletion mutant lost the ability (Fig. 7*A*, *right*). Association of JDP2 with the *BZLF1* promoter correlated with increased HDAC3 recruitment to the promoter (Fig. 7*A*). This HDAC3 recruitment by JDP2 correlated to reduced levels of histone H3 acetylation (Fig. 7*B*). To extend these results, endogenous JDP2 was knocked down by siRNA (Fig. 7*C*). Recruitment of endogenous HDAC3 to Zp was weak although appreciable in the si-control case, whereas treatment with si-JDP2 decreased the HDAC3 interaction with Zp (Fig. 7*C*). The reduction in HDAC3 recruitment by si-JDP2 caused increments in histone H3 acetylation levels (Fig. 7*D*). Furthermore, JDP2 association with HDAC3 was confirmed by immunoprecipitation (Fig. 7*E*). These results suggest that HDAC3 recruitment to Zp, which coincides with lower levels of acetylated histone H3, is efficiently mediated by JDP2 protein.

DISCUSSION

In this report, we document evidence that JDP2 is able to suppress transcription from Zp, thereby inhibiting the entire life cycle in lytic infection. Our results indicate that JDP2 binds to the ZII *cis*-element of the *BZLF1* promoter, which has been reported to interact with b-Zip type transcriptional factors, such as CREB, ATF, and AP-1. Despite the fact that JDP2 represses Zp via the ZII *cis*-element, introduction of a

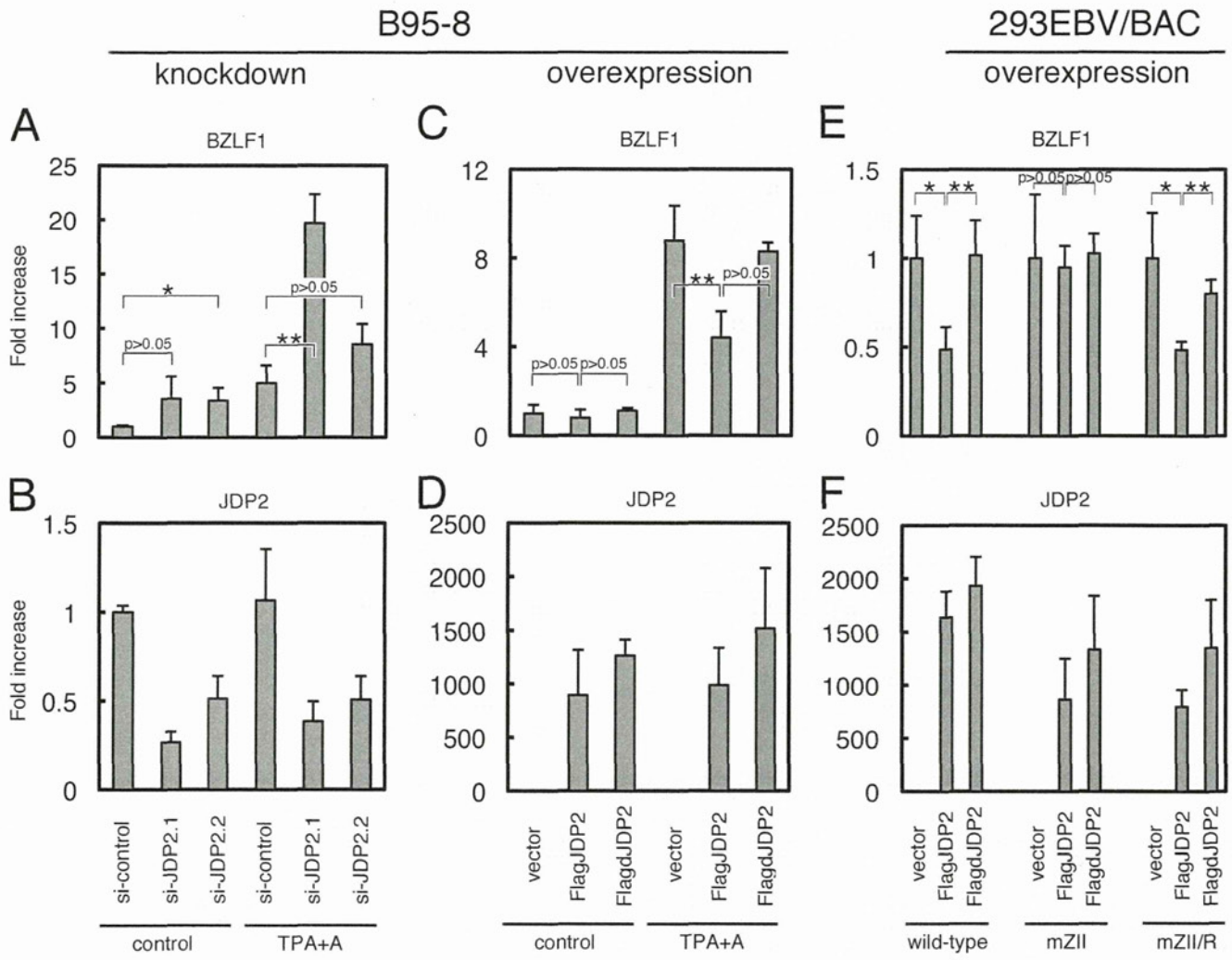

FIGURE 6. **JDP2 inhibits *BZLF1* expression.** *A* and *B*, knockdown of JDP2 enhances *BZLF1* expression. B95-8 cells transfected with siRNA against JDP2 (*si-JDP2.1* or *si-JDP2.2*) or a control (*si-control*) siRNA were cultured for 48 h, and then treated with TPA (20 ng/ml) and A23187 (1 mM) for an additional 12 h. Levels of *BZLF1* (*A*) and *JDP2* (*B*) were checked by real time RT-PCR. *C* and *D*, exogenous overexpression of JDP2 decreases *BZLF1* expression. B95-8 cells transfected with pCMV-FlagJDP2, pCMV-FlagdJDP2, which lacks b-Zip motif of JDP2, or the empty vector were cultured for 24 h, and then treated with TPA (20 ng/ml) and A23187 (1 mM) for an additional 12 h. Levels of *BZLF1* (*C*) and *JDP2* (*D*) were checked by real time RT-PCR. *E* and *F*, exogenous overexpression of JDP2 decreases *BZLF1* expression in HEK293 cells with recombinant EBV/BAC. Cells were transfected with pCMV-FlagJDP2, pCMV-FlagdJDP2, which lacks b-Zip motif of JDP2, or the empty vector. After 36 h, levels of *BZLF1* (*E*) and *JDP2* (*F*) mRNAs were quantified by real time RT-PCR. *BZLF1* and *JDP2* mRNA levels are normalized by *RNA polII* mRNA levels and shown as fold-activation of that for control (*leftmost bar*). * or ** indicates $p < 0.05$ or $p < 0.02$, respectively.

point mutation into the element did not activate BZLF1 expression. Instead, the mutation even reduced the basal expression of BZLF1 (Fig. 4*C*). We speculate that effects of the potential activators such as CREB, ATF, and AP-1 were more conspicuous than that of the negative regulator, JDP2 in the ZII element. Many reports have indicated a significance of the ZII domain for BZLF1 expression. For example, BZLF1 expression is highly leaky in AGS cells infected with EBV, at least partly due to abundant c-Jun and its binding to the ZII element (36). We are confident that JDP2 acts negatively on EBV reactivation, because knockdown of the gene substantially enhanced expression of viral immediate-early, early genes, and viral DNA replication (Fig. 6 and supplemental Fig. S4).

In Fig. 6, a huge amount (1,000-fold or even more of endogenous level of *JDP2*) of forced expression of JDP2 caused only 50% reduction in *BZLF1* mRNA levels. One might argue that this reduction must have been more extensive. We speculate that the ZII motif of the promoter might already be occupied by endogenous b-Zip transcription factors, including JDP2, and thus exogenously supplied JDP2 could not replace effectively. Otherwise, JDP2 might be just one of several proteins that serve to restrict the BZLF1 expression, and the restriction by JDP2 could easily be achieved by the presence of a relatively small amount of the protein.

Because JDP2 and viral BZLF1 are both b-Zip-type transcriptional factors, we tested if they could interact with each other. Immunoprecipitation assays clearly demonstrated that JDP2 and BZLF1 associated through their b-Zip elements (data not shown), and we thus examined if the factors could act cooperatively on the *BZLF1* promoter (Fig. 1). However, we observed no evidence of such cooperation, and the ZIII *cis*-element, the binding motif for BZLF1, did not appear to be involved in the suppression by JDP2 (Fig. 1).

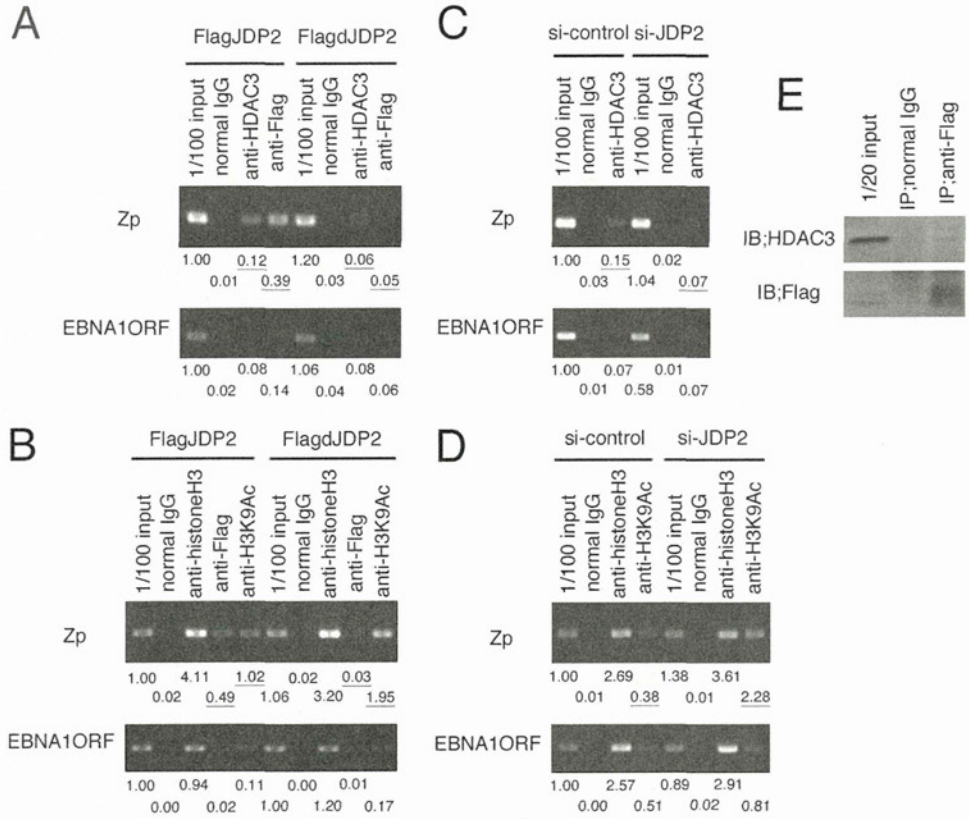

FIGURE 7. **JDP2 mediates HDAC3 recruitment to the *BZLF1* promoter.** *A* and *B*, HEK293 cells with wild-type EBV-BAC DNA were transfected with the FLAG-JDP2 expression vector (*FlagJDP2*) or the expression vector with a deletion in the b-Zip domain (*FlagdJDP2*). After 24 h, ChIP experiments were carried out using cross-linked DNA-protein complexes from the cells, precipitated using normal IgG, anti-HDAC3, anti-FLAG anti-histone H3, or anti-acetylated histone H3K9 antibody, followed by DNA extraction and PCR to detect the Zp. A fragment for the EBNA1 open reading frame was also detected as a control. *C* and *D*, HEK293 cells with wild-type EBV-BAC DNA were transfected with the siRNA against JDP2 (*si-JDP2.1*) or the control (*si-control*). After 48 h, ChIP experiments were carried out using normal IgG, anti-HDAC3 anti-histone H3, or anti-acetylated histone H3K9 antibody, followed by DNA extraction and PCR to detect the Zp and a fragment for the EBNA1 open reading frame as a control. The samples in *A–C* were also subjected to real time PCR analysis for quantification, and the relative values indicated *below* the bands. *E*, JDP2 associates with HDAC3. Proteins from HEK293T cells transfected with FLAG-tagged JDP2 expression vector were subjected to immunoprecipitation using normal IgG or mouse anti-FLAG monoclonal antibody followed by immunoblotting with rabbit anti-HDAC3 (*upper panel*) and rabbit anti-FLAG antibodies (*lower panel*).

Besides JDP2, several factors have been reported to suppress the *BZLF1* promoter. SMUBP-2, a transcription factor first identified through its interaction with the immunoglobulin Smu region, represses Zp activation by TPA (37). ZEB proteins restrict BZLF1 expression by binding to the ZV element of the promoter (38–40). E-box binding proteins, E2-2 (41), and Yin Yang1 (YY-1) (42) have also been implicated. Suppression by JDP2 is distinct from that of these factors, because it relies on binding to the ZII element. Identification and detailed analysis of negative regulators of *BZLF1* transcription should help to understand EBV reactivation mechanisms and provide a whole picture of the virus life cycle.

We found that the CMV promoter responded to JDP2 knockdown differently from the *BZLF1* promoter, although both were similarly suppressed by JDP2 overexpression (data not shown). We speculate that the affinity between the repressor and those promoters might vary. Aronheim's group (26) recently demonstrated that JDP2 activates transcription from TPA responsive element-dependent promoters through association with CHOP10, suggesting that JDP2 can be a transcriptional activator, as well, depending on the context. One possible hypothesis is that the CMV promoter might be regulated both positively and negatively by JDP2, and JDP2 knockdown act in both ways, whereas exogenous overexpression causes emphatic effects on the negative side. The reasons remain to be determined, but it is clear that JDP2 siRNA served, in this report, as the best tool to elucidate its biological roles under physiological conditions.

Knockdown of JDP2 by siRNA in EBV-positive Akata cells increased the levels of early gene expression and viral replication, when the viral lytic program was elicited by anti-IgG treatment (supplemental Fig. S4). Likewise, viral replication was augmented by such silencing in other cell lines, such as B95-8 and GTC-4 cells (data not shown), when treated with TPA and calcium ionophore. Interestingly, in EBV-positive HEK293 cells, knockdown of JDP2 still intensified viral lytic replication even when BZLF1 protein was exogenously supplied (data not shown). This result suggests that JDP2 can act at multiple steps in the lytic life cycle of the virus, and suppression at the *BZLF1* promoter is not the only inhibitory point.

In conclusion, we here have provided evidence that JDP2 is involved in regulation of the latent-lytic switch in EBV infection. Elucidation of associated factors may contribute to development of anti-EBV agents in the future.

Acknowledgments—We thank Drs. W. Hammerschmidt, H. J. Delecluse, K. Shimotohno, and A. Aronheim for providing the EBV-BAC system, HEK293 cells, expression vectors for CREB and c-Jun, and anti-JDP2 antibodies, respectively. XBP1 cDNA was a kind gift from Dr. K. Mori. We also express our appreciation to T. Gamano for technical assistance.

REFERENCES

1. Speck, S. H., Chatila, T., and Flemington, E. (1997) *Trends Microbiol.* **5,** 399–405
2. Amon, W., and Farrell, P. J. (2005) *Rev. Med. Virol.* **15,** 149–156
3. Tsurumi, T., Fujita, M., and Kudoh, A. (2005) *Rev. Med. Virol.* **15,** 3–15
4. Flemington, E., and Speck, S. H. (1990) *J. Virol.* **64,** 1217–1226
5. Liu, S., Liu, P., Borras, A., Chatila, T., and Speck, S. H. (1997) *EMBO J.* **16,** 143–153
6. Liu, S., Borras, A. M., Liu, P., Suske, G., and Speck, S. H. (1997) *Virology* **228,** 11–18
7. Liu, P., Liu, S., and Speck, S. H. (1998) *J. Virol.* **72,** 8230–8239
8. Ruf, I. K., and Rawlins, D. R. (1995) *J. Virol.* **69,** 7648–7657
9. Flemington, E., and Speck, S. H. (1990) *J. Virol.* **64,** 1227–1232
10. Aronheim, A., Zandi, E., Hennemann, H., Elledge, S. J., and Karin, M. (1997) *Mol. Cell. Biol.* **17,** 3094–3102
11. Ostrovsky, O., Bengal, E., and Aronheim, A. (2002) *J. Biol. Chem.* **277,** 40043–40054
12. Kawaida, R., Ohtsuka, T., Okutsu, J., Takahashi, T., Kadono, Y., Oda, H., Hikita, A., Nakamura, K., Tanaka, S., and Furukawa, H. (2003) *J. Exp. Med.* **197,** 1029–1035
13. Nakade, K., Pan, J., Yoshiki, A., Ugai, H., Kimura, M., Liu, B., Li, H., Obata, Y., Iwama, M., Itohara, S., Murata, T., and Yokoyama, K. K. (2007) *Cell Death Differ.* **14,** 1398–1405
14. Jin, C., Li, H., Murata, T., Sun, K., Horikoshi, M., Chiu, R., and Yokoyama, K. K. (2002) *Mol. Cell. Biol.* **22,** 4815–4826
15. Lerdrup, M., Holmberg, C., Dietrich, N., Shaulian, E., Herdegen, T., Jäättelä, M., and Kallunki, T. (2005) *Biochim. Biophys. Acta* **1745,** 29–37
16. Piu, F., Aronheim, A., Katz, S., and Karin, M. (2001) *Mol. Cell. Biol.* **21,** 3012–3024
17. Heinrich, R., Livne, E., Ben-Izhak, O., and Aronheim, A. (2004) *J. Biol. Chem.* **279,** 5708–5715
18. Blazek, E., Wasmer, S., Kruse, U., Aronheim, A., Aoki, M., and Vogt, P. K. (2003) *Oncogene* **22,** 2151–2159
19. Bitton-Worms, K., Pikarsky, E., and Aronheim, A. (2010) *Mol. Cancer* **9,** 54
20. Nakade, K., Pan, J., Yamasaki, T., Murata, T., Wasylyk, B., and Yokoyama, K. K. (2009) *J. Biol. Chem.* **284,** 10808–10817
21. Rasmussen, M. H., Sørensen, A. B., Morris, D. W., Dutra, J. C., Engelhard, E. K., Wang, C. L., Schmidt, J., and Pedersen, F. S. (2005) *Virology* **337,** 353–364
22. Hwang, H. C., Martins, C. P., Bronkhorst, Y., Randel, E., Berns, A., Fero, M., and Clurman, B. E. (2002) *Proc. Natl. Acad. Sci. U.S.A.* **99,** 11293–11298
23. Jin, C., Ugai, H., Song, J., Murata, T., Nili, F., Sun, K., Horikoshi, M., and Yokoyama, K. K. (2001) *FEBS Lett.* **489,** 34–41
24. Jin, C., Kato, K., Chimura, T., Yamasaki, T., Nakade, K., Murata, T., Li, H., Pan, J., Zhao, M., Sun, K., Chiu, R., Ito, T., Nagata, K., Horikoshi, M., and Yokoyama, K. K. (2006) *Nat. Struct. Mol. Biol.* **13,** 331–338
25. Wardell, S. E., Boonyaratanakornkit, V., Adelman, J. S., Aronheim, A., and Edwards, D. P. (2002) *Mol. Cell. Biol.* **22,** 5451–5466
26. Weidenfeld-Baranboim, K., Bitton-Worms, K., and Aronheim, A. (2008) *Nucleic Acids Res.* **36,** 3608–3619
27. Murata, T., Hotta, N., Toyama, S., Nakayama, S., Chiba, S., Isomura, H., Ohshima, T., Kanda, T., and Tsurumi, T. (2010) *J. Biol. Chem.* **285,** 23925–23935
28. Murata, T., Isomura, H., Yamashita, Y., Toyama, S., Sato, Y., Nakayama, S., Kudoh, A., Iwahori, S., Kanda, T., and Tsurumi, T. (2009) *Virology* **389,** 75–81
29. Murata, T., Sato, Y., Nakayama, S., Kudoh, A., Iwahori, S., Isomura, H., Tajima, M., Hishiki, T., Ohshima, T., Hijikata, M., Shimotohno, K., and Tsurumi, T. (2009) *J. Biol. Chem.* **284,** 8033–8041
30. Ego, T., Tanaka, Y., and Shimotohno, K. (2005) *Oncogene* **24,** 1914–1923
31. Matsumoto, J., Ohshima, T., Isono, O., and Shimotohno, K. (2005) *Oncogene* **24,** 1001–1010
32. Yoshida, H., Matsui, T., Yamamoto, A., Okada, T., and Mori, K. (2001) *Cell* **107,** 881–891
33. Nakayama, S., Murata, T., Yasui, Y., Murayama, K., Isomura, H., Kanda, T., and Tsurumi, T. (2010) *J. Virol.* **84,** 12589–12598
34. Delecluse, H. J., Hilsendegen, T., Pich, D., Zeidler, R., and Hammerschmidt, W. (1998) *Proc. Natl. Acad. Sci. U.S.A.* **95,** 8245–8250
35. Bhende, P. M., Dickerson, S. J., Sun, X., Feng, W. H., and Kenney, S. C. (2007) *J. Virol.* **81,** 7363–7370
36. Feng, W. H., Kraus, R. J., Dickerson, S. J., Lim, H. J., Jones, R. J., Yu, X., Mertz, J. E., and Kenney, S. C. (2007) *J. Virol.* **81,** 10113–10122
37. Zhang, Q., Wang, Y. C., and Montalvo, E. A. (1999) *Virology* **255,** 160–170
38. Yu, X., Wang, Z., and Mertz, J. E. (2007) *PLoS Pathog.* **3,** e194
39. Kraus, R. J., Perrigoue, J. G., and Mertz, J. E. (2003) *J. Virol.* **77,** 199–207
40. Ellis, A. L., Wang, Z., Yu, X., and Mertz, J. E. (2010) *J. Virol.* **84,** 6139–6152
41. Thomas, C., Dankesreiter, A., Wolf, H., and Schwarzmann, F. (2003) *J. Gen. Virol.* **84,** 959–964
42. Montalvo, E. A., Cottam, M., Hill, S., and Wang, Y. J. (1995) *J. Virol.* **69,** 4158–4165

JOURNAL OF VIROLOGY, July 2011, p. 6127–6135 Vol. 85, No. 13
0022-538X/11/$12.00 doi:10.1128/JVI.00258-11

Spatiotemporally Different DNA Repair Systems Participate in Epstein-Barr Virus Genome Maturation▽

Atsuko Sugimoto,[1,2] Teru Kanda,[1] Yoriko Yamashita,[3] Takayuki Murata,[1] Shinichi Saito,[1] Daisuke Kawashima,[1] Hiroki Isomura,[1] Yukihiro Nishiyama,[2] and Tatsuya Tsurumi[1]*

Division of Virology, Aichi Cancer Center Research Institute, Chikusa-ku, Nagoya 464-8681, Japan,[1] and Department of Virology[2] and Department of Pathology and Biological Responses,[3] Nagoya University Graduate School of Medicine, Shōwa-ku, Nagoya 466-8550, Japan

Received 4 February 2011/Accepted 4 April 2011

Productive replication of Epstein-Barr virus occurs in discrete sites in nuclei, called replication compartments, where viral DNA replication proteins and host homologous recombinational repair (HRR) and mismatch repair (MMR) factors are recruited. Three-dimensional (3D) surface reconstruction imaging clarified the spatial arrangements of these factors within the replication compartments. Subnuclear domains, designated BMRF1 cores, which were highly enriched in viral polymerase processivity factor BMRF1 could be identified inside the replication compartments. Pulse-chase experiments revealed that newly synthesized viral genomes organized around the BMRF1 cores were transferred inward. HRR factors could be demonstrated mainly outside BMRF1 cores, where *de novo* synthesis of viral DNA was ongoing, whereas MMR factors were found predominantly inside. These results imply that *de novo* synthesis of viral DNA is coupled with HRR outside the cores, followed by MMR inside cores for quality control of replicated viral genomes. Thus, our approach unveiled a viral genome manufacturing plant.

Epstein-Barr virus (EBV), a human lymphotropic herpesvirus with a linear double-stranded DNA 172 kb in length (2), infects resting B lymphocytes, inducing their continuous proliferation without production of virus particles, this being termed latent infection. Productive infection, which occurs spontaneously or can be induced artificially, is characterized by expression of lytic genes, leading to virus production. The EBV genome is amplified 100- to 1,000-fold by viral replication machinery composed of BALF5 DNA polymerase, BMRF1 polymerase processivity factor, BALF2 single-stranded-DNA (ssDNA) binding protein, and BBLF4-BSLF1-BBLF2/3 helicase-primase complex in discrete sites in nuclei, which are called replication compartments (9, 13). With progression of productive replication, the replication compartments become enlarged and fuse to form large globular structures that eventually fill the nucleus in late stages (9).

We have previously reported the architecture of the EBV replication compartments (9). The BZLF1 *oriLyt* binding proteins show a fine, diffuse pattern of distribution throughout the nuclei at immediate-early stages of induction and then become associated with the replicating EBV genome in the replication compartments during lytic infection. The BMRF1 proteins show a homogenous, not dot-like, distribution in the replication compartments, coinciding with the synthesized viral DNA. In contrast, the BALF5 Pol catalytic protein, the BALF2 single-stranded-DNA binding protein, and the BBLF2/3 protein, a component of the helicase-primase complex, were colocalized as distinct dots distributed within replication compartments, representing viral replication factories.

The BMRF1 protein is a major phosphoprotein abundantly expressed during EBV productive infection (7, 26), associating with the BALF5 polymerase catalytic subunit with one-to-one stoichiometry to enhance its polymerase processivity (41). Judging from immunostaining data, together with the finding that almost all expressed BMRF1 proteins bind to viral genome DNA, the factor has been assumed not only to act as a polymerase processivity factor but also to protect the viral genome after synthesis. In addition, it can transcriptionally activate the BHLF1 promoter (48) and enhance BZLF1-mediated transcription of the BALF2 promoter (33).

It has been suggested that DNA replication is coupled with DNA recombination to generate large branched head-to-tail concatemers of replication intermediates during herpesvirus genome replication (4, 44, 49). We previously showed that homologous recombinational repair (HRR) factors such as replication protein A (RPA), Rad51, Rad52, and the Mre11/Rad50/Nbs1 (MRN) complex are recruited and loaded onto the newly synthesized viral genome in replication compartments (23). HRR is an accurate repair process known to be mediated by the MRN complex, RPA, members of the RAD52 epistasis group of gene products such as Rad51, Rad52, and Rad54, and phosphorylated BRCA1 and BRCA2 (5, 24). Knockdown of RPA32 and Rad51 by RNA interference significantly prevents viral DNA synthesis (23), indicating an HRR involvement in viral DNA synthesis.

We have also previously demonstrated that proliferating cell nuclear antigen (PCNA), the PCNA loader complex (RF-C), and a series of mismatch repair (MMR) proteins such as MSH2, MSH6, MLH1, and PMS2 can be assembled to Epstein-Barr virus replication compartments (10). MMR works primarily to correct mutations by removing base-base and

* Corresponding author. Mailing address: Division of Virology, Aichi Cancer Center Research Institute, Kanokoden, Chikusa-ku, Nagoya 464-8681, Japan. Phone and fax: 81-52-764-2979. E-mail: ttsurumi@aichi-cc.jp.

▽ Published ahead of print on 13 April 2011.

small insertion-deletion mismatches that arise during DNA replication, and it is mediated by MSH heterodimers (MSH2-MSH3 and MSH2-MSH6) and MLH heterodimers (MLH1-PMS2 and MLH1-MLH3) (18, 20). PCNA, which was originally characterized as a DNA sliding clamp for replicative DNA polymerases, interacts with MSH2-MSH6 or MSH2-MSH3 complexes, searching for mispairs on newly replicated DNA (8, 14, 19). RF-C recruits PCNA (the clamp) and loads it onto DNA in the presence of ATP (clamp loading), with this being required for MMR (47).

In other herpesviruses such as herpes simplex virus type 1 (HSV-1) and human cytomegalovirus (HCMV), viral replication compartments are also formed in the infected nuclei during the productive replication, and HRR factors, including the MRN complex and Rad51, are reported to be recruited to the replication compartments (27, 29, 36, 37, 46). Furthermore, Taylor and Knipe reported that the HSV-1-encoded single-stranded-DNA binding protein ICP8 interacts either directly or indirectly with HRR and MMR factors (37). Also, HSV-1 alkaline exonuclease UL12 has recently been shown to interact specifically with the MRN complex (3).

Here we examined the spatial arrangements of viral DNA replication factors and cellular HRR and MMR factors in the replication compartments by means of confocal laser scanning microscopy and three-dimensional (3D) surface reconstruction imaging. BMRF1-rich subnuclear domains, designated BMRF1 cores, could be identified inside the replication compartments. As a result, each replication compartment was partitioned into two subdomains, outside and inside the BMRF1 core. We here present data demonstrating that viral DNA replication and viral genome maturation are assigned to outside and inside subdomains, respectively.

MATERIALS AND METHODS

Cell culture. Tet-BZLF1/B95-8 cells were maintained in RPMI 1640 medium supplemented with 1 μg/ml puromycin, 250 μg/ml hygromycin B, and 10% tetracycline-free fetal calf serum (Clontech) at 37°C in a humidified 5% CO_2 atmosphere. To induce lytic EBV replication, the tetracycline derivative doxycycline was added to the culture medium at a final concentration of 4 μg/ml. When blocking lytic replication, phosphonoacetic acid (PAA), a herpesvirus DNA polymerase-specific inhibitor, was added to the culture medium at a final concentration of 400 μg/ml.

Antibodies. Anti-BALF2 and anti-BMRF1 rabbit polyclonal antibodies were as previously prepared (10, 40, 42). Anti-BALF5 protein-specific rabbit antibodies (43) were affinity purified with BALF5 protein coupled-Sepharose 4B as described previously (15). An anti-EBV EA-D-p52/50 (BMRF1 gene product) protein-specific mouse monoclonal antibody, clone name R3, was purchased from Chemicon Inc. 5-Chloro-2′-deoxyuridine (CldU)-labeled DNAs were detected with anti-5-bromo-2′-deoxyuridine (anti-BrdU) rat monoclonal antibody clone BU1/75 (ICR1), purchased from Abcam. The anti-BrdU antibody clone BU1/75 (ICR1) does not cross-react with 5-iodo-2′-deoxyuridine (IdU). Anti-pRPA32 S4/S8, -BRCA1 S1524, and -Mre11 rabbit polyclonal antibodies were purchased from Abcam and anti-Rad52 antibodies from Cell Signaling. Anti-PCNA mouse monoclonal and rabbit polyclonal antibodies were purchased from Transduction Laboratories and Abcam, respectively, and anti-MSH2, -MSH3, and -MSH6 monoclonal antibodies were obtained from Transduction Laboratories and BD Biosciences. The secondary goat anti-rabbit, anti-rat, and anti-mouse IgG antibodies conjugated with Alexa 488 or 594, a Zenon mouse IgG labeling kit (Alexa 594), and a Zenon rabbit IgG labeling kit (Alexa 594) were obtained from Molecular Probes.

Immunofluorescence analysis. All staining procedures except for extraction and incubation with primary antibodies were carried out at room temperature. For immunofluorescence experiments, cells were washed with ice-cold phosphate-buffered saline (PBS) and extracted with 0.5% Triton X-100–mCSK buffer [10 mM piperazine-*N*,*N*′-bis(2-ethanesulfonic acid) (PIPES) (pH 6.8), 300 mM sucrose, 1 mM $MgCl_2$, 1 mM EGTA, 1 mM dithiothreitol, 1 mM phenylmethylsulfonyl fluoride, 0.5% Triton X-100) on ice for 10 min. Multiple protease inhibitors (Sigma; 25 μl/ml), 200 μM Na_3VO_4, and 20 mM NaF were also added to the buffer. Cells were fixed with 70% ethanol for 24 h at −20°C, washed with PBS containing 0.1% normal goat serum and 0.01% Tween 20, permeabilized with 0.5% Triton X-100 in PBS for 15 min, blocked for 1 h in 10% normal goat serum in PBS, and then incubated overnight with the primary antibodies diluted in PBS containing 0.1% normal goat serum and 0.01% Tween 20. The samples were then incubated for 1 h with secondary goat anti-rabbit, anti-rat, and anti-mouse IgG antibodies conjugated with Alexa Fluor 488 or 594. For MSH2, MSH3, and MSH6 staining, anti-MSH2, -MSH3, and -MSH6 antibodies were directly labeled with a Zenon tricolor mouse IgG1 labeling kit purchased from Molecular Probes. Also, for BALF2, BRCA1 S1524, and Rad52 staining, anti-BALF2, -BRCA1 S1524, and -Rad52 antibodies were directly labeled with a Zenon tricolor rabbit IgG1 labeling kit purchased from Molecular Probes. Cells were incubated with Alexa Flour 594-labeled anti-MSH2, -MSH3, -MSH6, -BALF2, -BRCA1 S1524, and -Rad52 antibodies for 45 min at room temperature and washed three times with PBS, followed by a second fixation with 4% paraformaldehyde solution in phosphate buffer for 15 min at room temperature. All the primary antibodies were employed at a 1:100 dilution, and the secondary antibodies were employed at a 1:500 dilution. All washes after antibody incubation were performed with PBS containing 0.1% normal goat serum and 0.01% Tween 20. The slides were mounted in ProLong Gold antifade reagent with 4′,6′-diamidino-2-phenylindole (DAPI) (Molecular Probes) and analyzed by fluorescence confocal microscopy. Laser scanning confocal fluorescence microscopic images were captured and processed using an LSM510 Meta microscope (Carl Zeiss MicroImaging, Inc.) with a plan-Apochromat 100×/1.4-numerical-aperture oil immersion objective.

Pulse-chase experiments. For CldU pulse-labeling, newly synthesized DNA was labeled by incubating lytic replication-induced Tet-BZLF1/B95-8 cells with 10 μM CldU added directly to the incubation medium for 10 min at 24 h postinduction. For the pulse-chase experiments, the cells were pulse-labeled with 10 μM CldU for 10 min at 24 h postinduction, and the CldU-containing medium was removed and replaced with new medium containing IdU to inhibit CldU incorporation to newly synthesized DNA. Cells were chased for 1 h prior to harvesting. Cells were washed with ice-cold PBS and extracted with 0.5% Triton X-100–mCSK buffer on ice for 10 min. Multiple protease inhibitors (Sigma; 25 μl/ml), 200 μM Na_3VO_4, and 20 mM NaF were also added to the buffer. Cells were then fixed with 70% ethanol for 24 h at −20°C and treated for 60 min with 2 N HCl containing 0.5% Triton X-100 to expose the incorporated CldU residues before blocking. The cells were washed twice with PBS and neutralized with 0.1 M sodium tetraborate, pH 9.0, for 5 min prior to immunofluorescence.

Fluorescence in situ hybridization. EBV bacterial artificial chromosome (BAC) DNA was labeled with digoxigenin (DIG) nick translation mix (Sigma) and used as a probe. First, cells were fixed in 4% paraformaldehyde and 70% ethanol. After digestion with RNase, cells were treated with 50% formamide in 2× SSC (1× SSC is 0.15 M NaCl plus 0.015 M sodium citrate), air dried, and immediately covered with a probe mixture containing 60% formamide in 2× SSC containing probe DNA (4 ng/μl), 12% dextran sulfate, and sheared salmon DNA (0.1 μg/μl). Probes and cells were simultaneously heated at 85°C for 5 min and incubated overnight at 37°C. After hybridization, specimens were washed at 45°C with 50% formamide in 2× SSC (three times for 3 min each), at 45°C with 2× SSC (three times for 3 min each), and at 65°C with 0.1× SSC for 10 min. After washing, specimens were blocked for 1 h in 5% milk in 4× SCC containing 1% bovine serum albumin (BSA) and then stained with anti-DIG sheep monoclonal antibodies in 4× SSC containing 1% BSA at 37°C for 30 min. After staining, specimens were washed at room temperature with 4× SSC, 0.1% Triton X-100 in 4× SSC, 4× SSC, and PN buffer (0.5 M Na_2HPO_4, 0.5 M NaH_2PO_4, 0.5% NP-40) (three times for 3 min each). Finally, cells were stained with anti-BMRF1 mouse monoclonal antibodies, mounted in ProLong Gold antifade reagent with DAPI (Molecular Probes), and analyzed by fluorescence confocal microscopy. Images were captured and processed using an LSM510 Meta microscope (Carl Zeiss MicroImaging, Inc.) with a plan-Apochromat 100×/1.4-numerical-aperture oil immersion objective.

3D reconstruction with confocal laser scanning microscopy. Images observed with a confocal laser scanning microscope (Carl Zeiss MicroImaging, Inc.) were computerized to automatically make 50 to 100 serial optical sections at intervals of around 0.26 μm. The 3D reconstruction was performed with Imaris software (Carl Zeiss MicroImaging, Inc.). Image files created by the LSM510 Meta microscope were opened with Imaris, and a 3D surface model was created based on the appropriate intensity threshold.

RESULTS

BMRF1-rich structures (cores) are observed in viral replication compartments. We previously described a B95-8 derivative cell line in which we can trigger onset of viral lytic replication via tetracycline-inducible expression of viral immediate-early protein BZLF1 (Tet-BZLF1/B95-8 cells) (22). In this study, we utilized Tet-BZLF1/B95-8 cells to examine more details of replication compartments during viral productive replication. The lytic replication-induced Tet-BZLF1/B95-8 cells were harvested and extracted with 0.5% Triton X-100–mCSK buffer. It should be noted that the treatment extracts soluble viral or cellular proteins, permitting investigation of DNA-bound fractions of viral and cellular proteins. We tested for specificity of the secondary antibodies and for reliability of discrimination with the fluorescence microscopy filters. When cells were stained singly for either antigen with inappropriate combinations of first and second antibodies, no fluorescence was observed. Also, no immunofluorescence was observed with an alternate filter. We have previously defined EBV replication compartments as BMRF1- or BALF2-staining sites where viral DNA genomes are colocalized as judged by immunofluorescence and fluorescence *in situ* hybridization (FISH) analysis (9). A representative image of a viral replication compartment is illustrated in Fig. 1A, visualized by means of indirect immunofluorescence analyses. As shown in a merged image, BALF2 protein dots were distributed not only inside but also outside BMRF1-stained subnuclear domains. A correlative immunofluorescence microscopy and electron microscopic imaging (FM-EM) study found that BMRF1 proteins were localized within an electron-lucent region in the nuclear interior, in contrast with electron-dense chromatin regions (data not shown). At higher magnification, the area corresponding to the replication compartment contained diffuse noncondensed fibers and granules but lacked any specific structures.

In an independent experiment, the localizations of viral genome DNA and BMRF1 protein were simultaneously examined by means of combinational FISH and immunofluorescence. As shown in a representative image (Fig. 1B), the majority of viral genome DNA was localized inside BMRF1-localized regions. To support FISH analysis, we performed pulse-labeling analysis combined with immunofluorescence staining. The labeling reagent CldU, a nucleotide analog like BrdU, was added to the culture medium at 24 h postinduction and left for 10 min so that newly synthesized viral DNAs were labeled with incorporated CldU. As shown in Fig. 1C, CldU staining coincided with BMRF1- and BALF2-localized regions. In the presence of PAA, a herpesvirus DNA polymerase-specific inhibitor, CldU and BMRF1 signals were not observed (Fig. 1C). In the presence of the inhibitor, viral replication compartments are not formed and the expressed BMRF1 proteins are solubilized by the detergent treatment, while BALF2 proteins are distributed throughout nuclei as distinct spots (9). Overall, these results indicate that viral genome DNA is synthesized in the replication compartments, confirming the previous observations (9).

Spatial localization of viral replication proteins within replication compartments. Confocal images are frequently presented as brightest point projections, but this format is not appropriate for demonstrating the spatial distribution of objects. To establish spatial relationships among viral replication proteins within replication compartments, 3D surface reconstruction imaging was employed. We used a 3D visualization and volume modeling software program, Imaris, to create images. We first examined the spatial distribution of BMRF1 relative to viral ssDNA binding protein BALF2 and viral DNA polymerase BALF5. Our previous work demonstrated colocalization of BALF5 with BALF2 as distinct spots within replication compartments, with the two proteins most likely cooperatively working at viral replication forks (9). As illustrated in a representative 3D image (Fig. 2A), each mass of BMRF1 protein appeared to be surrounded by BALF2 protein. We named the BMRF1-rich structures "BMRF1 cores." It should be noted that BALF2 protein also localized inside the BMRF1 core, as observed in 2D images (Fig. 2A). Similarly, as shown in another representative 3D surface reconstruction image (Fig. 2B), each BMRF1 core was surrounded by BALF5 DNA polymerase, although BALF5 was also localized inside the BMRF1 core as shown in the 2D image (Fig. 2B). On the other hands, the BALF5 and BALF2 proteins colocalized well both outside and inside the BMRF1 core (Fig. 2). From the 3D

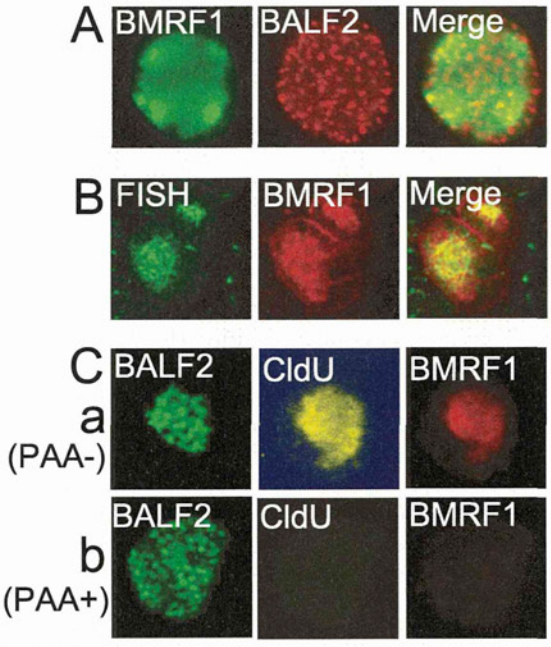

FIG. 1. The majority of viral genome DNA is localized inside BMRF1-rich structures. (A) Lytic replication-induced Tet-BZLF1/B95-8 cells were fixed, stained with anti-BMRF1 (green) and anti-BALF2 (red) antibodies, and observed by laser scanning confocal microscopy to locate viral replication compartments. The right panel is a merged image. (B) Lytic replication-induced Tet-BZLF1/B95-8 cells were fixed in 4% paraformaldehyde and 70% ethanol. After digestion with RNase, they were treated with 50% formamide, air dried, and immediately hybridized with a mixture containing the EBV BAC DNA probe labeled with DIG nick translation mix. Specimens were stained with fluorescein isothiocyanate (FITC)-conjugated anti-DIG sheep (green) and anti-BMRF1 mouse (red) monoclonal antibodies. The right panel is a merged image. (C) Newly synthesized DNAs were labeled by incubation with 10 μM CldU added directly to the culture medium of lytic replication-induced Tet-BZLF1/B95-8 cells for 10 min at 24 h postinduction in the presence (b) or absence (a) of PAA (400 μg/ml). Specimens were stained with anti-BALF2 (green), anti-CldU (yellow), and anti-BMRF1 (red) antibodies.

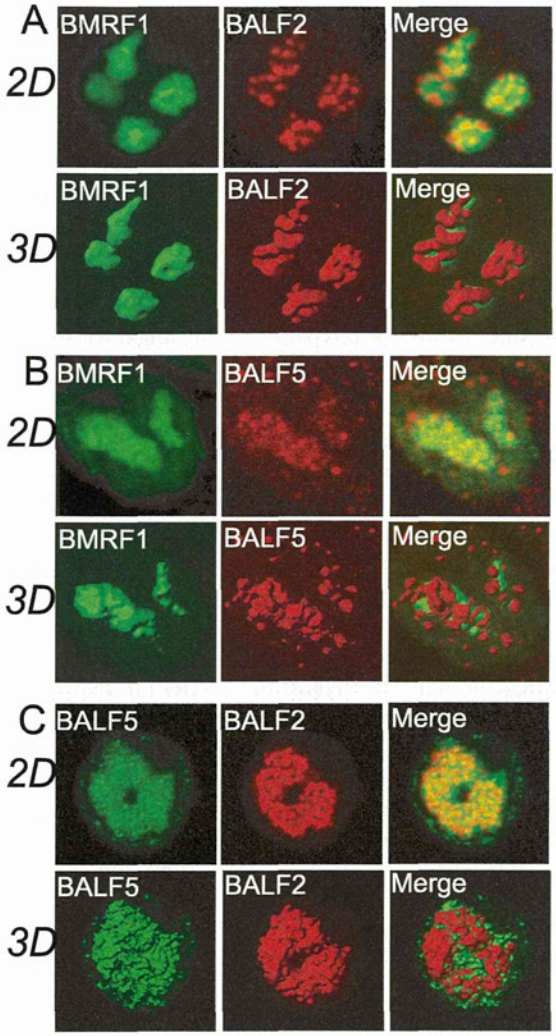

FIG. 2. 3D surface reconstruction imaging of viral replication compartments. (A) Laser scanning confocal images of BMRF1 and BALF2 proteins. Lytic replication-induced Tet-BZLF1/B95-8 cells were treated with 0.5% mCSK buffer, fixed with 70% ethanol, and stained with anti-BMRF1 (green) and anti-BALF2 (red) antibodies. The 2D images show brightest-point projections of 60 images collected at 0.26-μm steps in the *z* axis. The same data are displayed as 3D topographical reconstructions of BMRF1 and BALF2 proteins (left and middle panels, respectively). The right panel shows a 3D surface reconstruction image of both proteins showing the BMRF1 core covered by BALF2 proteins. (B) Laser scanning confocal images of BMRF1 (green) and BALF5 (red) proteins. The 2D images show brightest-point projections of 60 images collected at 0.26-μm steps in the *z* axis. The same data are displayed as 3D topographical reconstructions of BMRF1 and BALF5 proteins (left and middle panels, respectively). The right panel shows a 3D surface reconstruction image of both proteins showing the BMRF1 core covered by BALF5 Pol proteins. (C) Laser scanning confocal images of BALF5 (green) and BALF2 (red) proteins. The 2D images show brightest-point projections of 60 images collected at 0.26-μm steps in the *z* axis. The same data are displayed as 3D topographical reconstructions of BALF5 and BALF2 proteins (left and middle panels, respectively). The right panel shows a 3D surface reconstruction image of both proteins, showing that the BALF5 Pol proteins and BALF2 proteins are mingled.

surface reconstruction image it appeared that both proteins are mingled on their surfaces (Fig. 2C).

Viral DNA genomes newly synthesized outside the BMRF1 core move to the inside. We have previously demonstrated that the sites stained with anti-BMRF1 protein-specific antibodies coincided with the foci of 1-h-pulse-labeled viral DNA as judged by 5-bromodeoxyuridine (BrdU) incorporation and FISH analyses on confocal immunofluorescence analyses and that the BrdU-pulse-labeled DNA moved out of nucleus with time, clarifying that BrdU-labeled DNAs at 24 h postinduction are mostly viral and not cellular DNAs (10).

Our observation that the BMRF1 core was surrounded by a BALF2 ssDNA binding protein and the BALF5 DNA polymerase protein, whereas the majority of viral genomes were inside the core, let us hypothesize that viral DNAs are synthesized outside cores and then transported inside. This hypothesis fits well with the idea that BMRF1, a viral polymerase processivity factor, also protects newly synthesized viral genomes during lytic replication. To test the hypothesis, we performed pulse-chase labeling experiments to monitor the location of newly synthesized viral DNAs. The labeling reagent CldU, a nucleotide analog like BrdU, was added to cells at 24 h postinduction and left for 10 min so that newly synthesized viral DNAs were labeled with incorporated CldU. As shown in a representative image (Fig. 3A), pulse-labeled newly synthesized viral DNAs were localized mainly outside the BMRF1 core, although some existed inside. In contrast, when 1 h of chasing was included after CldU pulse-labeling, all of the labeled viral DNAs were localized inside the BMRF1 core (Fig. 3B). From the 3D surface reconstruction image it appeared that the BALF2 protein and pulse-labeled DNA were mingled (Fig. 3A, bottom panels). These results correspond well with the idea that BMRF1 protein assembles on newly synthesized DNAs to form the cores, and the cores progressively enlarge during the course of productive infection.

HRR proteins are recruited to outside and inside BMRF1 cores. We have previously reported that homologous recombinational repair (HRR) factors such as replication protein A (RPA), Rad51, Rad52, and the Mre11/Nbs1/Rad50 (MRN) complex are recruited and loaded onto the newly synthesized viral genome in replication compartments (23). Therefore, we determined the spatial localization of the HRR factors within these compartments. As shown in a representative image (Fig. 4A), Mre11, a component of the MRN complex, covered and also existed inside the BMRF1 cores. It is noteworthy that the spatial localization of Mre11 (Fig. 4A) resembles that of newly synthesized viral DNAs (Fig. 3A, pulse-labeling without chasing). Similarly, BRCA1, Rad52, and phosphorylated RPA32 at Ser-4/-8 covered the cores (Fig. 4B, C, and D), again resembling the localization of newly synthesized viral DNAs (Fig. 3A). Figure 4D shows relative localizations of BMRF1, BALF2, and phosphorylated RPA (pRPA) within the replication compartment of the same cell. BALF2 and pRPA were colocalized and surrounded the BMRF1 core. This observation corresponds well with our previous demonstration that knockdown of RPA32 and Rad51 by RNA interference significantly prevented viral DNA synthesis (23) and supports the idea that HRR somehow contributes to coordinated viral DNA replication.